

A retrospective and prospective examination of the 1960s U.S. Northeast Drought

Zeyu Xue¹ and Paul Ullrich²

¹University of California, Davis

²University of California Davis

November 26, 2022

Abstract

As the most severe drought over the Northeastern United States (NEUS) in the past century, the 1960s drought had pronounced socioeconomic and natural impacts. Although it was followed by a persisting wet period, the conditions leading to the 1960s extreme drought could return in the future, along with its challenges to water management. To project the characteristics and potential consequences of such a future drought, pseudo-global warming simulations using the Weather Research and Forecasting Model are performed to simulate the dynamical conditions of the historical 1960s drought, but with modified thermodynamic conditions under the RCP8.5 scenario in the early (2021-2027), middle (2041-2047) and late (2091-2097) 21st century. Our analysis focuses on essential hydroclimatic variables including temperature, precipitation, evapotranspiration, soil moisture, snowpack and surface runoff. In contrast to the historical 1960s drought, similar dynamical conditions will generally produce more precipitation, increased soil moisture and evapotranspiration, and reduced snowpack. However, we also find that although wet months get much wetter, dry months may become drier, meaning that wetting trends are most significant in wet months but are essentially negligible for extremely dry months with negative monthly mean net precipitation. For these months, the trend towards wetting conditions provides little relief from the effects of extreme dry months. These conditions may even aggravate water shortages due to an increasingly rapid transition from wet to dry conditions. Other challenges emerge for residents and stakeholders in this region, including more extreme hot days, record-low snow pack, frozen ground degradation and subsequent decreases in surface runoff.

Hosted file

supporting information_pgw paper_zeyu xue.docx available at <https://authorea.com/users/554919/articles/605806-a-retrospective-and-prospective-examination-of-the-1960s-u-s-northeast-drought>

1 **A retrospective and prospective examination of the**
2 **1960s U.S. Northeast Drought**

3 **Zeyu Xue¹ and Paul Ullrich¹**

4 ¹Atmospheric Science Graduate Group, University of California, Davis, Davis, California

5 **Key Points:**

- 6 • Returned 1960s droughts are simulated under warming climate in the early, mid-
7 dle and late century.
8 • A significant wetting trend emerges; however, it helps little to mitigate the extreme
9 dry months.
10 • Significant snowpack loss and surface runoff decrease are anticipated for future droughts.

Corresponding author: Zeyu Xue, zyxue@ucdavis.edu

Abstract

As the most severe drought over the Northeastern United States (NEUS) in the past century, the 1960s drought had pronounced socioeconomic and natural impacts. Although it was followed by a persisting wet period, the conditions leading to the 1960s extreme drought could return in the future, along with its challenges to water management. To project the characteristics and potential consequences of such a future drought, pseudo-global warming simulations using the Weather Research and Forecasting Model are performed to simulate the dynamical conditions of the historical 1960s drought, but with modified thermodynamic conditions under the RCP8.5 scenario in the early (2021-2027), middle (2041-2047) and late (2091-2097) 21st century. Our analysis focuses on essential hydroclimatic variables including temperature, precipitation, evapotranspiration, soil moisture, snowpack and surface runoff. In contrast to the historical 1960s drought, similar dynamical conditions will generally produce more precipitation, increased soil moisture and evapotranspiration, and reduced snowpack. However, we also find that although wet months get much wetter, dry months may become drier, meaning that wetting trends are most significant in wet months but are essentially negligible for extremely dry months with negative monthly mean net precipitation. For these months, the trend towards wetting conditions provides little relief from the effects of extreme dry months. These conditions may even aggravate water shortages due to an increasingly rapid transition from wet to dry conditions. Other challenges emerge for residents and stakeholders in this region, including more extreme hot days, record-low snow pack, frozen ground degradation and subsequent decreases in surface runoff.

Plain Language Summary

The 1960s Northeastern United States (NEUS) drought was an abnormally long period of subnormal precipitation with subsequent impacts on water supply, partly countered by its cold temperatures. Under a changing climate, risks persist for returned conditions that drove this historically extreme drought. To project the potential impacts of a reoccurred 1960s drought, this study employs a climate modeling methodology known as pseudo-global warming. This approach aims at representing historical weather events under a warming climate. Results show that under similar dynamical conditions, the NEUS will overall be much wetter with more net precipitation and soil moisture. But these wet conditions do not manifest in all months; wetting trends are only apparent in wet and moderate months. For extreme dry months with historically negative net precipitation, net precipitation is largely unchanged and may even decrease slightly. Future precipitation variability increases and drought tends to initiate faster. Additional challenges arise with more extreme hot days, more severe extreme precipitation, less snowpack, frozen ground degradation and subsequent surface runoff decrease. This research provides extensive projections of hydrometeorological conditions under a warming climate that is valuable to water managers, policymakers and stakeholders to ensure they are informed of hydrometeorological risks brought by changing climate.

1 Introduction

Both historical observations and climate predictions indicate that climate change is likely to increase the intensity and frequency of extreme weather events such as droughts, floods, wildfires and heatwaves (Kharin et al., 2007; Hayhoe et al., 2007; Pfahl et al., 2017). Among these, droughts are one of the costliest natural disasters, with the most severe droughts having economic impacts greater than \$10 billion dollars (Andreadis & Lettenmaier, 2006). However, significant uncertainties persist regarding droughts' frequency and magnitude in a warming climate (Strzepek et al., 2010). Consequently there's an increasing and unmet need for understanding how such extreme droughts respond to climate change.

61 The Northeastern United States (NEUS) is the most economically developed and
62 populated region in the US, accounting for about 20% of US GDP and population but
63 only 5% of its land area (Hobbs, 2008; of Economic Analysis, 2016). Here, extreme weather
64 events – primarily floods, droughts and snowstorms – result in disproportionate socioe-
65 conomic damage. One of the most well known examples of extreme weather in this re-
66 gion was the 1962-66 drought, which had pronounced implications for agriculture and
67 water management practices (Namias, 1966; Barksdale, 1968; Janes & Brumbach, 1965).
68 Although the direct economic damage was not extensive (DeGaetano, 1999), this event
69 has since framed water resource planning in the NEUS. Consequently, a return of the
70 water stresses from this period would have enormous implications. To this end, it im-
71 portant to understand how would such an extreme drought’s characters change under
72 future climatological conditions? Notably, the unprecedented 1960s drought was followed
73 by a long wet period that continued through today (Seager et al., 2012). Both histor-
74 ical observations and climate models show continued increase in precipitation over NEUS
75 (Frumhoff et al., 2007); however, this should not imply that droughts here are things of
76 the past. In fact, there is evidence that the risk of potentially even more severe droughts
77 remains (Frumhoff et al., 2007; Burns et al., 2007; Hayhoe et al., 2007). Advances in cli-
78 mate models have made it possible to improve our confidence in these projections, and
79 so it is timely to revisit the nature of drought in this region.

80 Pseudo-global warming (PGW) is a demonstrably effective method for simulating
81 the effects of global warming. This method not only reduces large-scale model biases and
82 ensures that dynamical conditions are consistent with a historical analogue, but also al-
83 lows us to directly estimate differences between current and future climatological condi-
84 tions (Ullrich et al., 2018; Kimura et al., 2007). Using PGW, global climate model (GCM)
85 projections are used to modify the meteorological boundary conditions of the historical
86 1961-1967 period to reflect the impact of climate change on dry and moderate periods,
87 and speculate on the characteristics of such an extreme drought at the beginning-of-century
88 (2021-2027), mid-century (2041-2047) and end-of-century (2091-2097). This study thus
89 focuses on how the dynamical conditions of this period would manifest in a warming cli-
90 mate.

91 This paper focuses on trends in hydroclimatic variables and the consequences for
92 society and agriculture. Perhaps the most obvious trend being that there will be signif-
93 icant warming, which is observed to be particularly strong over the wintertime at higher
94 latitudes. This causes a decrease in the number of freezing days, early spring snowpack
95 melt and areas of seasonally frozen ground essentially disappearing by the end-of-century.
96 Further, this warming drives a surge in the number of extreme hot days (those with re-
97 gional mean heat index larger than 41°C). Even with subsequent increases in evapotran-
98 spiration, net precipitation increases over most of the NEUS. Using 24-month long-term
99 standardized precipitation index (SPI24) of net precipitation we project mean meteo-
100 rological conditions of these future drought analogues to be nearly normal, wet and ex-
101 tremely wet at the beginning, middle and end-of-century. However, the short-term SPI
102 (SPI1) of net precipitation indicates this general wetting trend is primarily manifest dur-
103 ing moderate months, and so net precipitation variability increases and is responsible
104 for exacerbating the discrepancy between dry and moderate periods. By end-of-century,
105 an extreme drought could potentially develop in only one month from extremely wet con-
106 ditions.

107 Other risks also emerge that threaten water resources in this region. For instance,
108 unprecedented extreme precipitation events will emerge during moderate periods. The
109 99th percentile of precipitation will increase by more than 50% by the end-of-century
110 compared with analogous years in the 1960s. Widespread flood events are expected to
111 become more frequent, and are likely to impact aging infrastructure. Further, early melt
112 of snowpack will lead to less runoff recharge in the early spring. And degradation of frozen
113 ground will lead to more infiltration of water from surface runoff to soil. In conjunction,

114 by end-of-century these factors will reduce March surface runoff to below half of histor-
 115 ical levels, with impacts for the growing season. These changes have likely consequences
 116 for both ecosystems and agriculture in the region.

117 **2 The record-setting 1960s drought**

118 The 1960s drought, which occurred from late 1962 to 1966, has been deemed as the
 119 most severe drought in the Northeastern US over last century. Its prominence in the re-
 120 gion's water resource planning emphasizes that drought is not only limited to commonly
 121 dry regions (Barksdale, 1968; Janes & Brumbach, 1965; Seager et al., 2012; Cook & Ja-
 122 coby, 1977; Lyon et al., 2005). The drought affected millions of people, and covered an
 123 area from New England to Virginia and from the Atlantic Coast to Ohio (Barksdale, 1968).
 124 As seen in Figure 1, meteorological dryness was the primary driver of the drought, as
 125 temperatures were anomalously low over this period (Namias, 1966). These low temper-
 126 atures spared the region from potentially more severe impacts (Namias, 1966; Janes &
 127 Brumbach, 1965). In the New England Region, negative Palmer Drought Severity In-
 128 dex (PDSI) values, associated with drought conditions, began in 1962 and ended at 1966;
 129 however, 1962's annual average PDSI was nearly 0 as the drought's effects only mani-
 130 fested in the latter half of the year. Therefore, in this paper, we refer to the years 1963-
 131 1966 as "dry" years and 1961, 1962 and 1967 as "moderate" years. This distinction is
 132 important as we will contrast future impacts for dry and moderate periods. The most
 133 negative PDSI and lowest soil moisture level of the climatological record occurred in 1965,
 134 exemplifying the intensity of the drought and the importance of 1965 as the year with
 135 the most pronounced impacts. Therefore, our study uses 1965 as the exemplar dry year
 136 and 1961, a year with the largest positive precipitation anomaly of the 1960s, as the ex-
 137 emplar moderate year. Notably, the 1960s drought was at its most severe in the spring,
 138 and was driven by precipitation suppression from a low pressure anomaly over the North
 139 Atlantic Ocean and a descending, northerly flow over the NEUS (Namias, 1966; Seager
 140 et al., 2012).

141 At the beginning of 1962, there was little indication that the NE was descending
 142 into a drought state. Precipitation in the early spring of this year was nominal, but af-
 143 ter the 6 months of below-average precipitation that followed, a water shortage gradu-
 144 ally began to emerge that depleted the soil being used for irrigation (Barksdale, 1968).
 145 By late 1962, most observations of runoff and groundwater were below normal levels, and
 146 pronounced impacts to agricultural productivity were being felt in states like New York
 147 (Barksdale et al., 1966).

148 Dryness persisted beyond 1962, and although heavy precipitation occurred in late
 149 1963 and early/late 1964, outside of the growing season this did little to prevent the spread
 150 of drought (Barksdale, 1968). Consequently, the growing season of 1964 was recorded
 151 as the driest of the last century (Janes & Brumbach, 1965). The drought intensified fur-
 152 ther in 1965 and spread over a wider swath of the northeast. Besides limiting water use,
 153 the drought also had an impact on water quality (Barksdale, 1968), as previously un-
 154 used and polluted water sources began being used to counter water shortages. Rivers'
 155 pollutant concentration increased due to insufficient dilution, and sea water intrusion threat-
 156 ened coastal freshwater quality.

157 Strict rules on water conservation and better management helped greatly in man-
 158 aging the water shortage from 1965 to 1966. Several new regulations were introduced
 159 that included prohibitions on washing of automobiles and urban irrigation. At last, the
 160 drought ended with abundant precipitation in September 1966 (Barksdale, 1968), with
 161 regional mean PDSI rising above zero for the first time in four years.

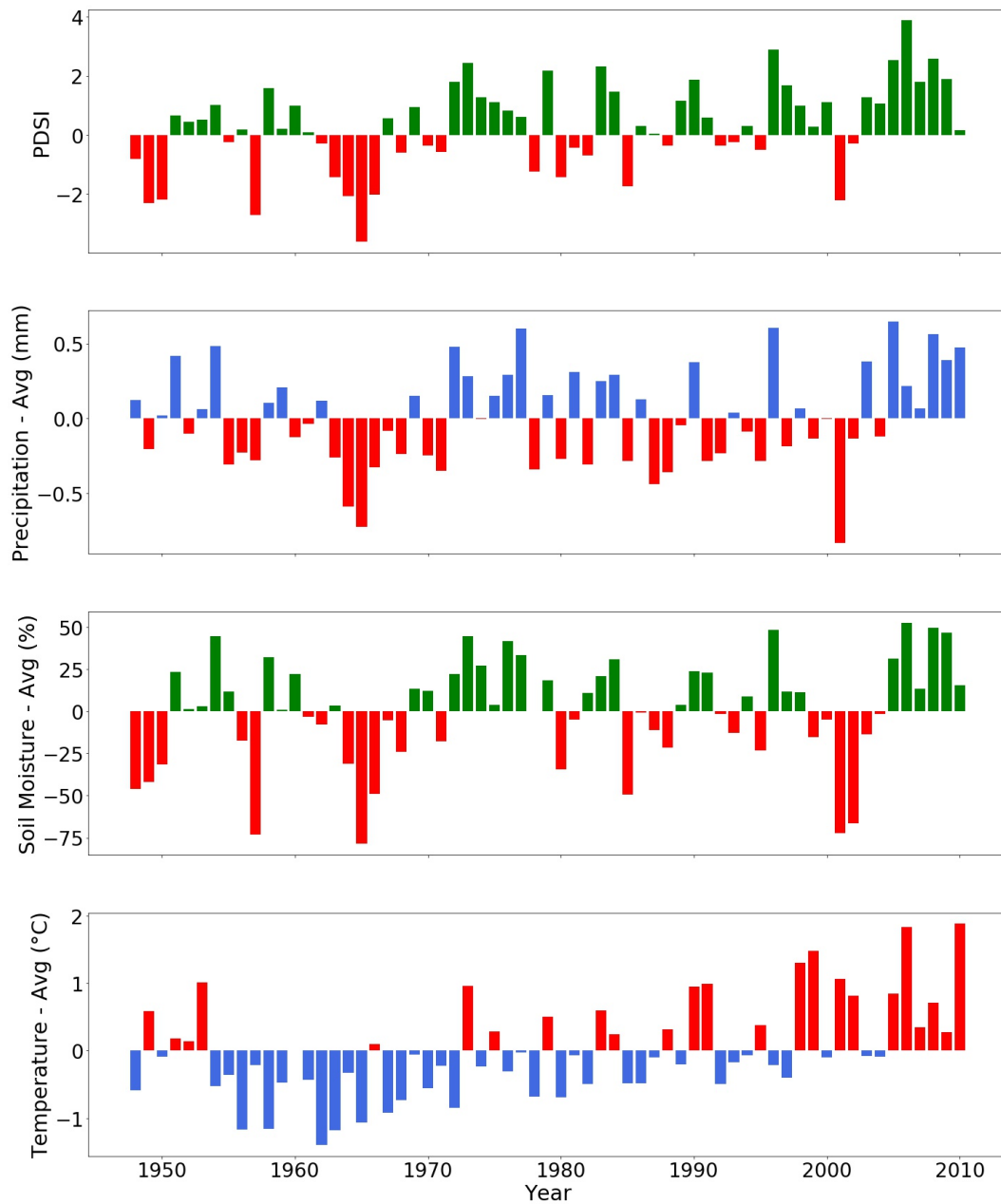


Figure 1. Palmer Drought Severity Index (PDSI) and the anomalies of precipitation, temperature and soil moisture from 1948 to 2010 over the New England Region. PDSI data from NCAR (Dai et al., 2004). Soil moisture data from PSL (Van den Dool et al., 2003). Precipitation and temperature from CERA20C R7 (European Centre for Medium-Range Weather Forecasts, 2016).

3 Uncertainty of a return to drought conditions under climate change

Large uncertainty remains for future trends of drought in the NEUS. Studies generally conclude that although the region is becoming wetter, drought – especially short-term drought – will occur more frequently and intensely under climate change (Frumhoff et al., 2007; Hayhoe et al., 2008; Demaria et al., 2016). Nonetheless, drought is an emergent feature that is affected by changes in thermodynamics (e.g. increases in atmospheric water vapor), hydrology (e.g. precipitation phase, runoff, related land surface variables, and surface-atmosphere fluxes) and dynamical conditions (shifts in the frequency, intensity or duration of meteorological patterns). Overall, both historical observations and model projections indicate an upward trend in average temperature ($0.3^{\circ}\text{C}/0.5^{\circ}\text{F}$ per decade since 1970, with wintertime warming of $0.7^{\circ}\text{C}/1.3^{\circ}\text{F}$ per decade) and a slight increase in average runoff and evapotranspiration (Hayhoe et al., 2007; Frumhoff et al., 2007; Seager et al., 2012). This has meant more extreme heat days, early melt dates, a lower snowfall-rainfall ratio, and a longer growing season along with more water demand (Frumhoff et al., 2007; Seager et al., 2012; Burns et al., 2007; Hayhoe et al., 2007). Although increased precipitation has meant that drought indices such as SPEI and SPI are shifting towards more positive values, indicative of generally wetter conditions, the spread of these indices is also increasing; consequently, the probability of extreme drought is largely unchanged in both observational data and models (Krakauer et al., 2019).

Water resource planning in the NEUS is highly reliant on a model drought based off of the 1960s drought period. Given subsequent climatic shifts (and foreseeable climatic shifts), there are concerns with the use of a model drought from more than a half century ago (Moser et al., 2008). Consequently, NEUS water management agencies agree that this model drought should be revisited in light of climate change. In the future, earlier snowmelt dates and reduced wintertime snowpack will certainly impact seasonal availability of water (Frumhoff et al., 2007; Burns et al., 2007; Huntington et al., 2004). Future warming will lead to a longer growing season and enhanced evaporation, thus enhancing consumption of available freshwater, particularly in spring and summer (Seager et al., 2012; Frumhoff et al., 2007; Lyon et al., 2005). While the 1960s drought is notable for its severe water shortage in these seasons, its socioeconomic impacts were also tempered by low temperatures. Capturing these factors under climate change motivates the use of a comprehensive model-based study of this period.

4 A simulation of present and future analogues of the 1960s drought

Having motivated the purpose of our study, we now present our methodology and results from our simulations using pseudo-global warming, including temperatures, precipitation, evapotranspiration, snowpack, soil moisture, runoff, and drought indices.

4.1 Methodology

In this study the Weather Research and Forecasting (WRF) Model is used for simulating the regional atmosphere of the NEUS (Skamarock et al., 2008; Powers et al., 2017). WRF is one of the most commonly-employed regional climate modeling systems currently available, incorporating many widely-recognized physical parameterizations. Thousands of research studies have been conducted with WRF worldwide, demonstrating WRF's utility for robust simulation of regional climate. With an appropriate choice of parameterizations, WRF has been shown in past studies to accurately reproduce the hydroclimatology of the NEUS (Ganetis & Colle, 2015). In this study WRF 3.9.1 is used with the parameterization suite given in Table 4.1. The land surface model employed is the Community Land Model 4 (CLM 4) (Oleson et al., 2010), which is the most complicated and expensive of the available options in WRF, but one that shows reasonable performance across a variety of geographies (Ullrich et al., 2018; Jin et al., 2010; Case et al., 2008).

Table 1. Physical parameterizations used in our WRF simulations.

Process	Parameterization
Microphysics	CAM V5.1 two-moment five-class (Neale et al., 2010)
Radiation	RRTMG (Iacono et al., 2008)
Surface layer	Revised MM5 similarity theory (Jiménez et al., 2012)
Land surface model	CLM4 (Oleson et al., 2010)
Planetary boundary layer	UW (Bretherton & Park, 2009)
Cumulus parameterization	ZM (G. J. Zhang & McFarlane, 1995)

212

4.1.1 *Simulation period and domain*

213

214

215

216

217

218

219

220

221

222

Our simulations in this paper cover four time periods: historical (1960-1967), present-day (2020-2027), mid 21st century (2040-2047) and late 21st century (2090-2097). In each simulation the first year serves as the spin-up period to ensure hydrologic and meteorological conditions have stabilized. Two nested domains are used (Figure 2). The outer and inner domains have 105×89 and 187×133 grid points, with resolutions of 18 and 6 km, respectively. Due to the long duration of the simulation, spectral nudging is employed (with the default relaxation timescale) so as to reduce internal model drift. In our simulations the 30-arc second (~ 1 km) resolution United States Geological Survey-based land use and land cover and topography datasets are interpolated to the model grids as geographical input.

223

224

225

226

Although most of our analysis focuses on the inner domain (Figure 2), some detailed analyses are conducted within the southern New England subregion (defined as 41N to 43N latitude and 74W to 70W longitude). This location comprises the most populated and developed areas of the NEUS.

227

4.1.2 *Modified forcing from pseudo-global warming*

228

229

230

231

232

233

234

235

236

237

Lateral forcing data for this historical period is from the 6-hourly Coupled ECMWF Re-Analysis system of the 20th-century (CERA-20C) R7 interpolated to 0.5° resolution. CERA-20C is a coupled reanalysis dataset with global coverage from 1901-2010, designed to capture low-frequency climate variability (European Centre for Medium-Range Weather Forecasts, 2016). This dataset is chosen because of its relatively high spatial and temporal resolution, and because its precipitation amounts best match observations of mean precipitation over the NEUS. After comparing the performance across all 10 CERA-20C ensembles, we selected the CERA-20C R7 ensemble as it again provided the highest performance among ensembles. More details on the evaluation protocol are provided in the Supporting Information Text S1.

238

239

240

241

242

243

244

245

246

247

248

Anticipated future changes to lateral forcing under climate change are derived from Coupled Model Intercomparison Project phase 6 (CMIP6) projections. In this study we use data from the multi-model mean of four CMIP6 models with demonstrably good performance in the NEUS region (namely, CESM2, MRI-ESM2-0, CNRM-ESM2-1 and GFDL-CM4), as identified by (Srivastava et al., 2020). Following (Ullrich et al., 2018), the spatially averaged monthly mean projections are used to calculate the difference between each of the 2020s, 2040s, and 2090s periods against the 1960s period. Both temperature and relative humidity are assessed in this manner. The resulting temperature differences as a function of month and altitude are depicted in Figure S1. We observe a positive temperature delta throughout the troposphere (up to around 100 hPa altitude), with a local maximum occurring around 350 hPa over the summer, and at the surface over win-

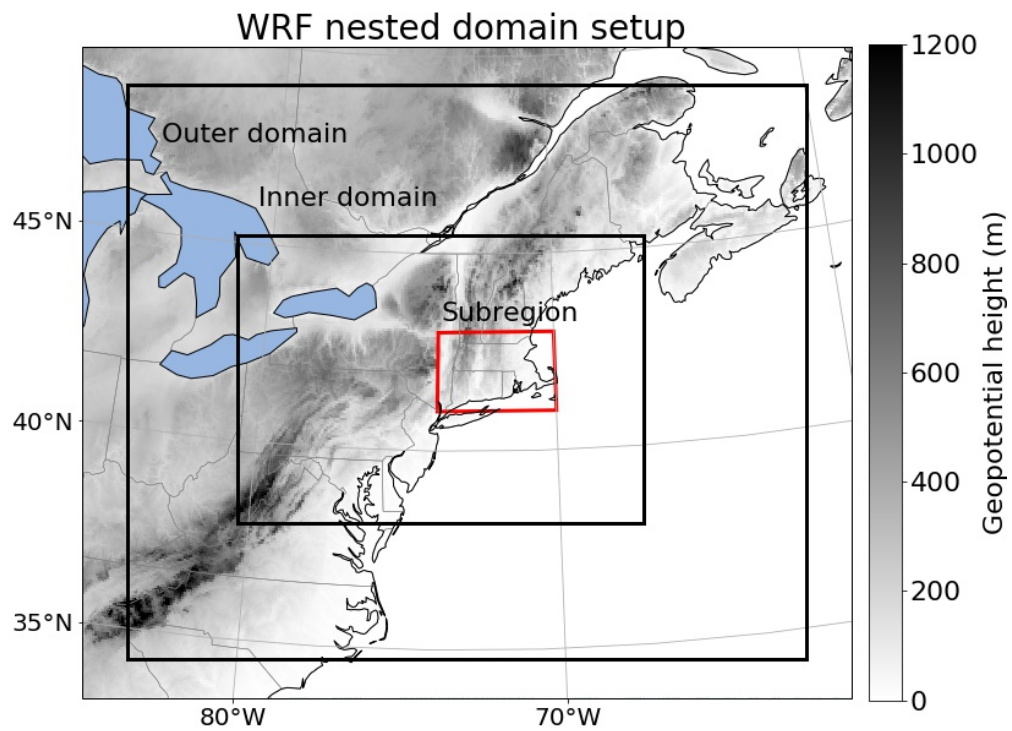


Figure 2. Our WRF domain setup for all simulations in this study. Shading indicates the surface height. Grid spacing in the outer (inner) domain is 18 km (6 km).

249 ter. There is a negative temperature delta in the stratosphere, as anticipated under cli-
 250 mate change. The magnitude of the temperature delta (both positive and negative) clearly
 251 increases from the 2020s to the 2040s and the 2090s, although the patterns are consis-
 252 tent. Relative humidity differences are small and so are not shown.

253 Lateral forcing data for the future simulations are the same as historical, except
 254 with the temperature delta (Figure S1) added over the entire domain, on constant pres-
 255 sure surfaces. Based on our observation of essentially negligible changes in relative hu-
 256 midity, relative humidity is held fixed (resulting in enhancement to specific humidity).
 257 Sea surface temperatures are analogously modified using the multi-model mean of the
 258 selected CMIP6 models to accord with the change to air temperatures. Finally, green-
 259 house gas concentrations are modified in WRF's radiation parameterization in accordance
 260 with the RCP8.5 emission scenario.

261 4.2 Annual mean temperature and precipitation percentiles

262 Simulated annual mean temperature and precipitation over our subregion for each
 263 year of the drought period is depicted in Figure 3 where historical data comes from CERA20C
 264 R7 and simulations are corrected by the regional mean difference between historical data
 265 (1961-1967) and WRF 1960s simulation. This plot also gives us a quick glimpse of how
 266 the climate of this region is projected to change: Whereas all years of the 1960s were be-
 267 low the 50th percentile of precipitation and most were below the 50th percentile of tem-
 268 perature, each simulated year of the 2040s and 2090s is above the 99.9th percentile of
 269 temperature, and all years of the 2090s are well above the 95th percentile of precipita-
 270 tion. This figure clearly highlights the significant regional shift towards a future warmer
 271 and wetter climate.

272 4.3 Temperature

273 From the CMIP model ensemble, the average warming rate over land from the 1960s
 274 period to 2090s period is 0.052°C per year, which is higher than the observed global warm-
 275 ing rate over land and ocean since 1981 (0.018°C per year) (Lindsey & Dahlman, 2020).
 276 Simulated warming of this magnitude is not unreasonable, as warming is expected to be
 277 much stronger over land and at higher latitudes (Hoegh-Guldberg et al., 2018). Figure
 278 4 shows the spatial pattern of 2m temperature from historical and its corresponding change.
 279 In general the magnitude of warming intensifies from the 2020s drought to the 2040s and
 280 the 2090s droughts, in accordance with expectations from the CMIP6 models under RCP8.5.
 281 However, the spatial and seasonal distributions of warming are uneven, with a stronger
 282 warming trend in winter (DJF) and at higher latitudes, where historical temperatures
 283 are lower; for example, regional mean change over land in 2045 DJF (4.14°C) is 1.52°C
 284 larger than 2045 JJA (2.62°C). From Figure 5, a clear correlation between future 2m tem-
 285 perature change and historical mean temperature at each grid point emerges, with en-
 286 hancement of the change in the winter season and under increased forcing; for example,
 287 the correlation over the 2095 winter (-0.62) is much larger than over the 2095 summer
 288 (-0.53), the winter of 2045 (-0.50), and the winter of 2025 (-0.43). This trend suggests
 289 that cold regions will be warming faster than warm regions, indicative of some homog-
 290 enization of temperatures over seasons and regions. Thus temperature spatial and tem-
 291 poral variability are reduced, in turn driving earlier snowmelt and intensified evapotran-
 292 spiration.

293 Do these trends also hold for moderate periods? Although the lateral temperature
 294 deltas of both the dry periods (1963-1966) and moderate periods (1961, 1962 and 1967)
 295 are the same, the simulations produce greater regional warming during moderate peri-
 296 ods than dry periods (although the difference is small). Further, some differences in spa-
 297 tial distribution of temperature change persist: From Figure 4 (fourth row), we can see
 298 that during the moderate wintertime period, the regions with highest temperature change

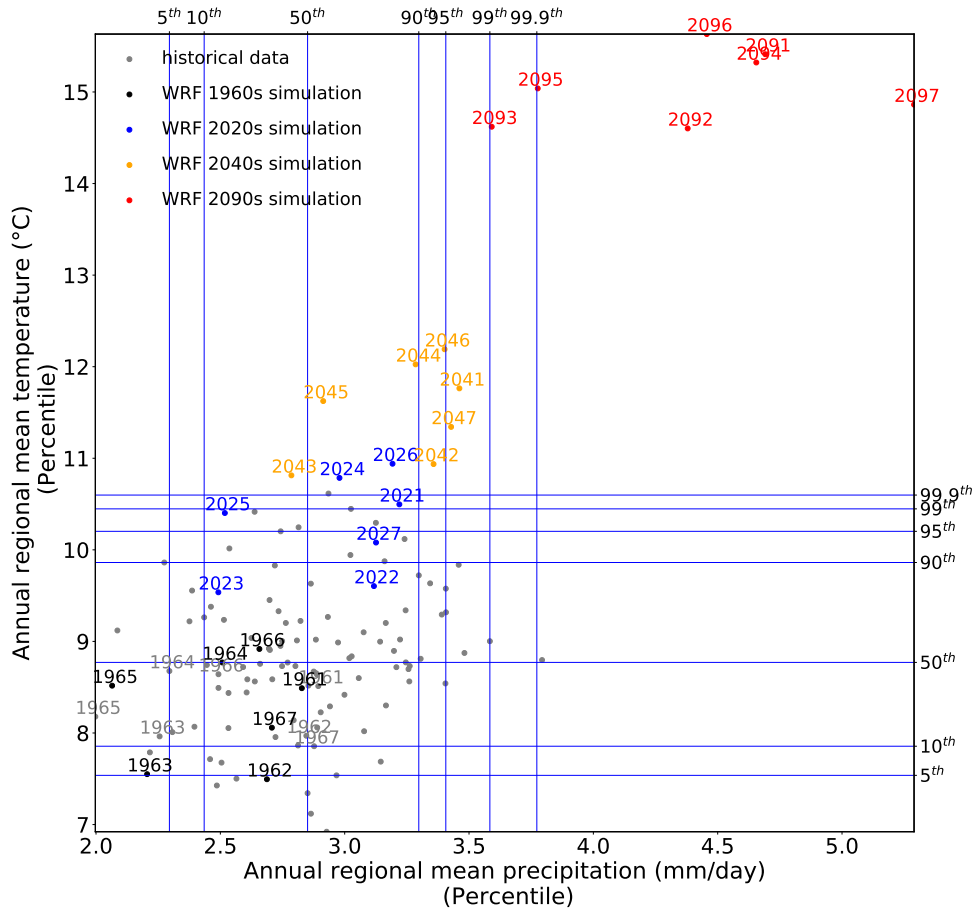


Figure 3. Regional annual mean precipitation and 2 meter temperature within the subregion during historical and future periods, as compared with historical percentiles over the period from 1910 to 2010.

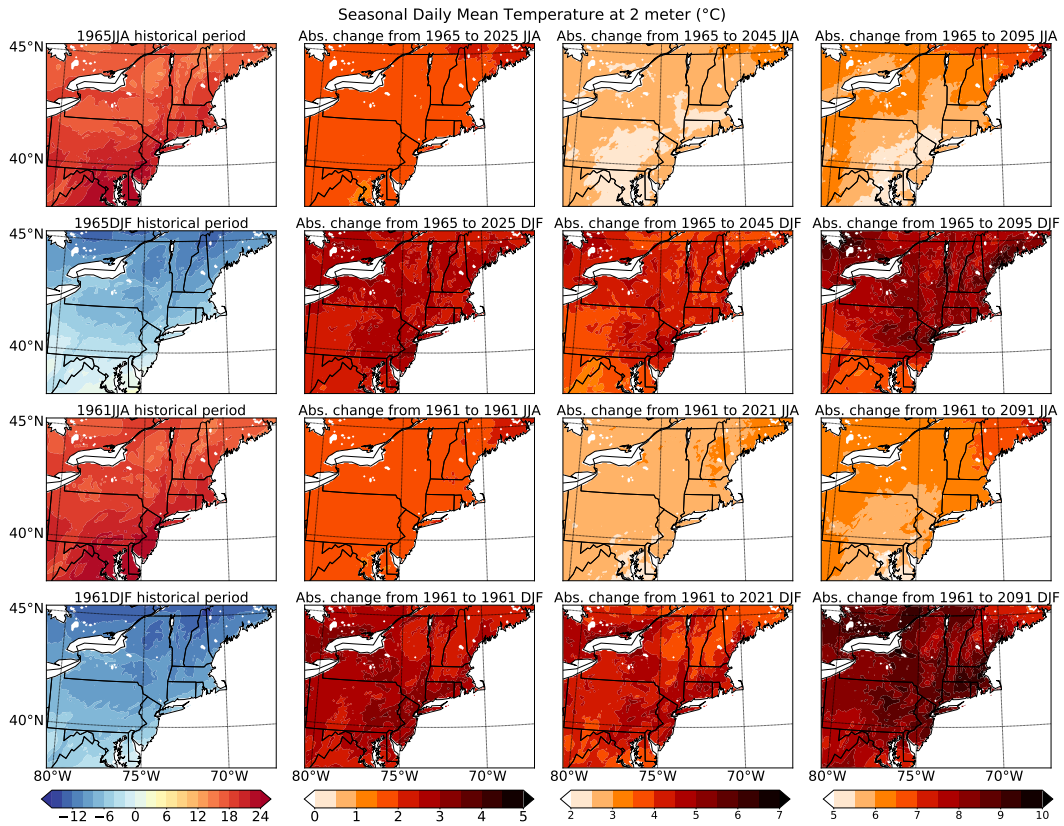


Figure 4. Average daily 2m temperatures (in degrees Celsius) over June-July-August (JJA) and December-January-February (DJF) in 1965 and 1961 (and their future analogues), exemplary of dry and moderate years.

299 are along the southern extent of New England; however, dry years have the greatest warm-
 300 ing along northern extent of the New England (Figure 4, second row). These wintertime
 301 spatial differences have consequences for dry years and non-dry years, such as shifts in
 302 the number of freezing days and snowmelt (touched on later).

303 **4.3.1 Extreme temperatures**

304 It is well known that shifts in mean temperatures will have a disproportionate influ-
 305 ence on the frequency of extreme temperatures. From figure 6, there is a clear increase
 306 in the mean annual maximum 2m temperature at all grid points, with more extremely
 307 hot days in the future; however, there is essentially no change in the annual variance of
 308 temperatures. With that said, both the mean and outliers of annual maximum daily tem-
 309 perature increase more in dry years rather than moderate years, which consequently drives
 310 an increase in evaporation and risk of flash drought. Frequency of extreme heat days are
 311 assessed using the Heat Index (HI) (Rothfusz & Headquarters, 1990) to better distin-
 312 guish extremely hot days with potential for significant socioeconomic impact (see Sup-
 313 porting Information Text S2 for the detailed definition of the Heat Index).

314 As defined by NOAA, values of HI larger than 41°C indicate dangerously hot condi-
 315 tions which may trigger sunstroke, heat cramps and heat exhaustion (NOAA, 2020).
 316 Figure 7 shows changes in the number of extreme heat days for each period for the sub-
 317 region. Compared with historical conditions (noting that this was a relatively cool pe-

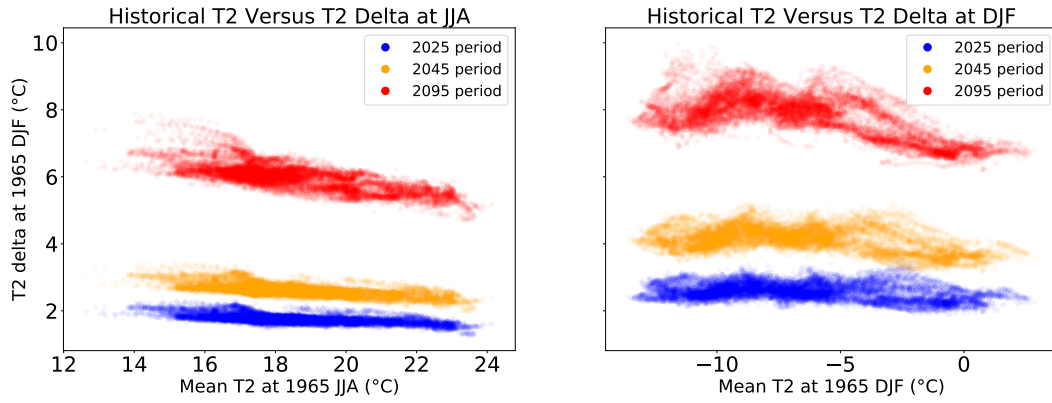


Figure 5. The relationship between historical mean daily 2m temperatures and future 2m temperatures deltas over JJA and DJF in 1965 drought conditions.

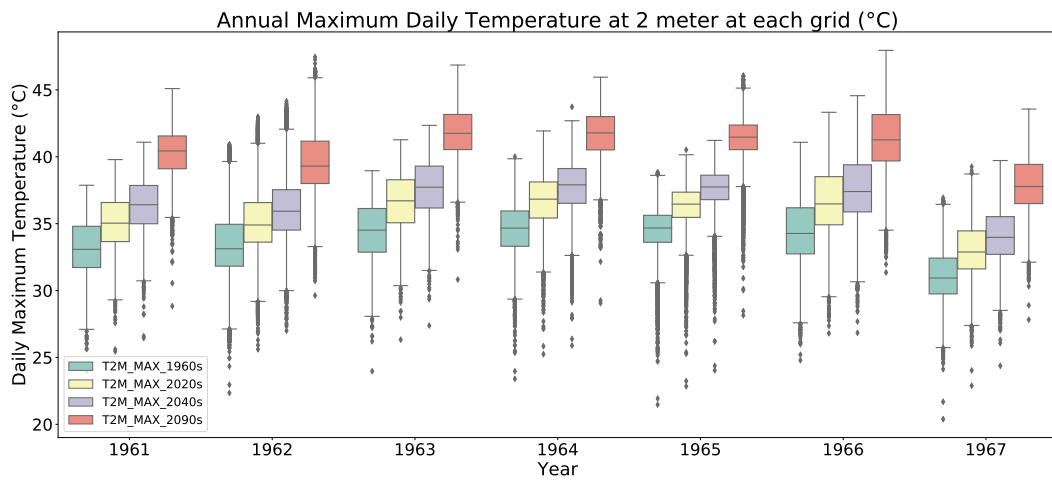


Figure 6. Annual maximum daily 2m temperature (in degrees Celsius) at each grid point.

318 rid), the number of extreme hot days increases from 6 in 1965 to 27 in 2045 and 56 at
 319 2095. It's clearly the case that extreme heat will be a major public health concern in the
 320 NEUS going forward.

321 The warming climate will also reduce the number of freezing days (days with daily
 322 2m temperature minimum less than 0°C) significantly in both dry year and moderate
 323 year (Figure 8). The change in freezing days is highly correlated with change in winter-
 324 time T2 (Figure 4). Further, the spatial distributions of the change in freezing day count
 325 differs significantly between our exemplar dry year (1965) and moderate year (1961), in
 326 accord with their associated temperature deltas and historical number of freezing days.
 327 Higher latitudes produce greater decreases of freezing days, where historical freezing days
 328 are more common and warming is larger. In these regions, we thus expect degradation
 329 of frozen ground (T. Zhang et al., 2003), which we will revisited later.

330 4.4 Precipitation

331 Figure 9 depicts seasonal mean daily precipitation over the historical and projected
 332 periods. Increasing precipitation is apparent in most regions, especially along the south-
 333 eastern coasts during winter and in the southwest during summer. These increases are

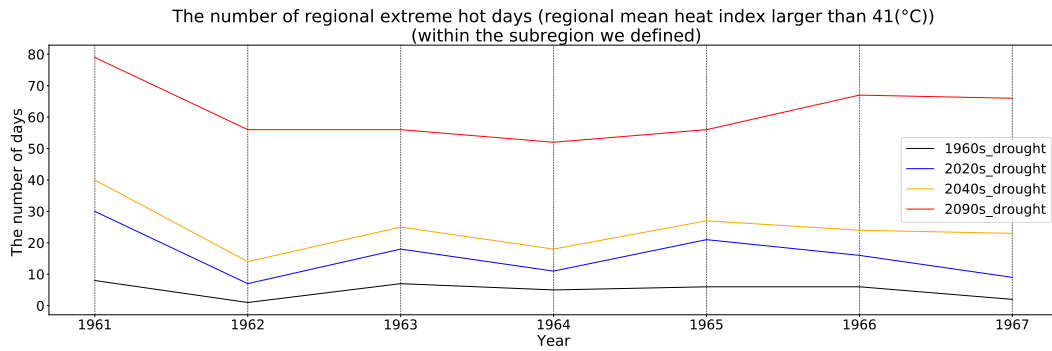


Figure 7. The number of regional mean extreme heat days (regional mean Heat Index larger than 41°C) for the historical period and each future analogue.

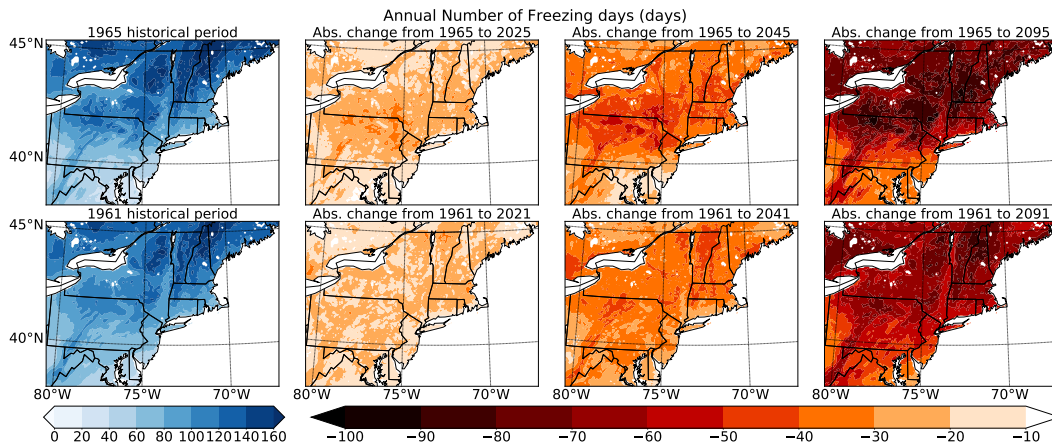


Figure 8. The number of freezing days in 1965 and 1961 (and their future analogues), defined by daily minimum 2m temperature less than 0°C.

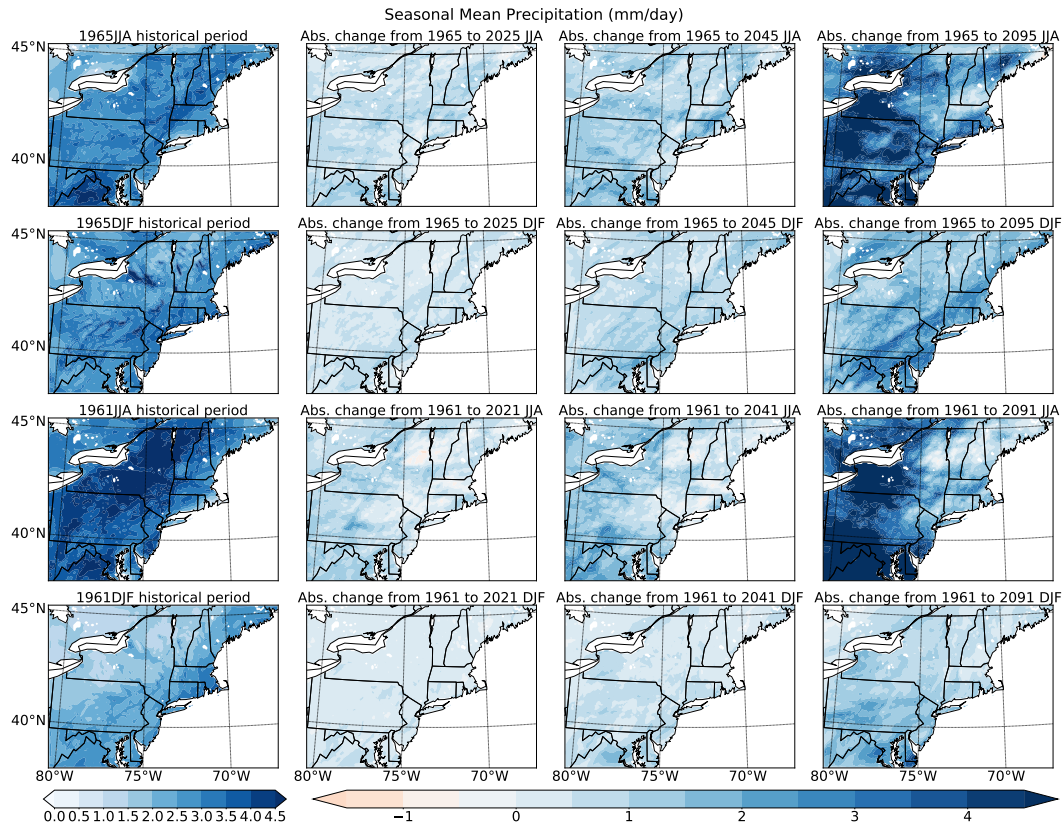


Figure 9. Seasonal mean precipitation distribution and change in the exemplar 1965 dry year and 1961 moderate year (mm/day).

334 expected because of an intensified hydrological cycle in the warming climate (Huntington
 335 et al., 2004; Pfahl et al., 2017). In the literature, the rule-of-thumb of warming climates
 336 ‘wet becomes wetter’ (Donat et al., 2016; Chou & Neelin, 2004; Seager et al., 2010) has
 337 been often employed to explain precipitation change over the ocean (Byrne & O’Gorman,
 338 2015); nonetheless, it also applies here (especially in the winter season). In Figure 9 re-
 339 gions with greater precipitation increase coincide with regions of larger historical mean
 340 wintertime precipitation, with pattern correlation in 2025 DJF, 2045 DJF and 2095 DJF
 341 of 0.51, 0.55 and 0.50, respectively (Figure S6). This result also applies for all other dry
 342 and moderate years, with even higher correlations of 0.8 in some cases (e.g. 2043 and
 343 2093 DJF). The applicability of this rule of thumb to the inland NEUS is likely a conse-
 344 quence of a relative abundance of water vapor in the region from the Atlantic Ocean
 345 and Gulf of Mexico. What’s more, unlike the dry period, the moderate period doesn’t
 346 experience more precipitation in the northeastern part of the inner domain; however, as
 347 we will discuss later, this region experiences a significant soil moisture increase during
 348 the moderate period.

349 Although this study is focused on drought, the dramatic increase in future precipi-
 350 tation deserves some discussion. Extreme precipitation is notorious for its disastrous im-
 351 pacts on society, and has been increasing in frequency across the continental US. This
 352 increase is particularly pronounced over the NEUS (Huntington et al., 2004; Hayhoe et
 353 al., 2007), where the most intense daily precipitation events (99th percentile daily pre-
 354 cipitation) have increased by more than 70% from 1958 to 2012 (Melillo et al., 2014).
 355 Our simulations also indicate that more extreme precipitation events will occur here in
 356 the future. Figure 10 shows that both absolute and relative precipitation percentiles will

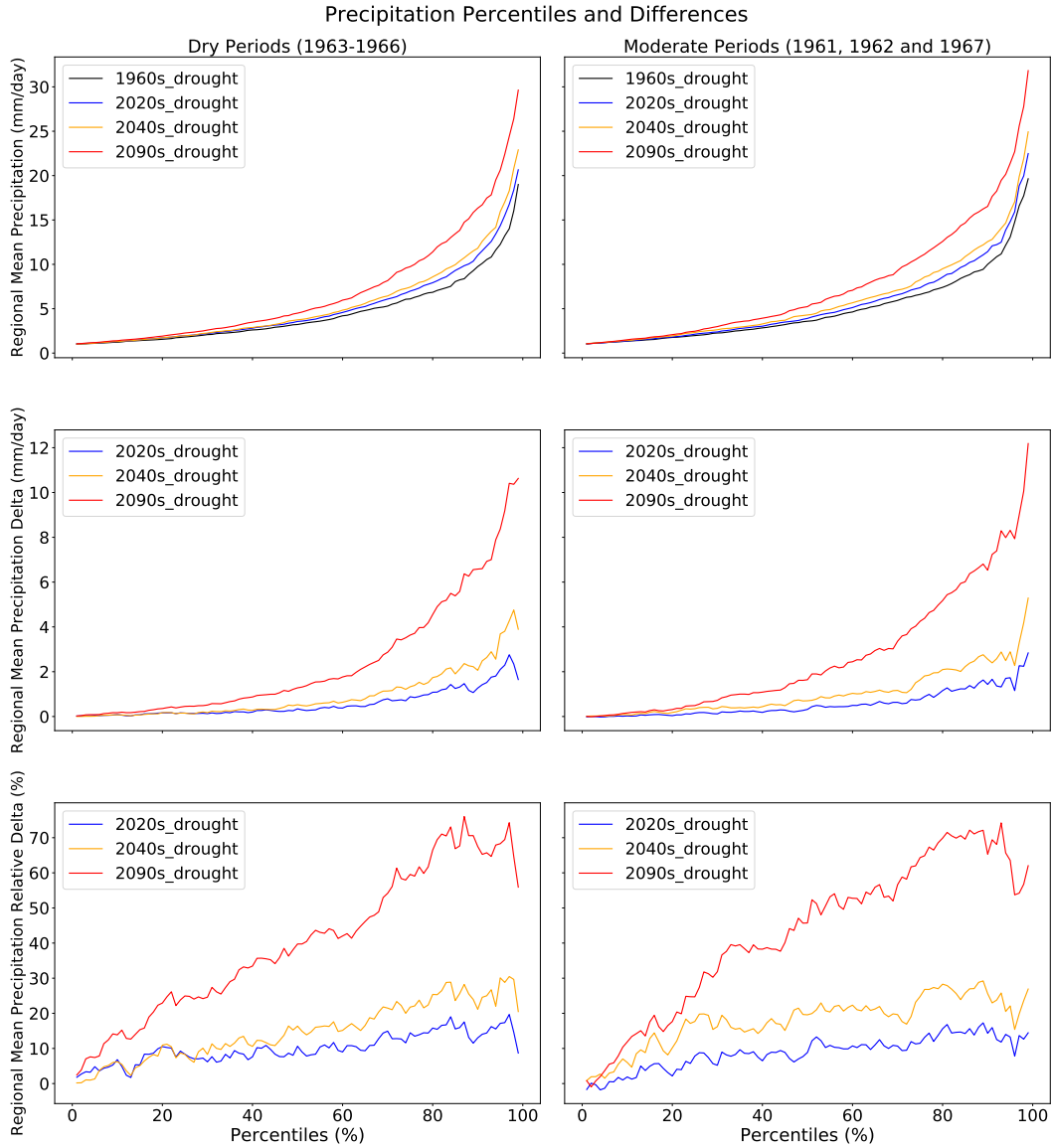


Figure 10. Regional mean precipitation change at different percentiles. Only daily precipitation events larger than 1 mm/day are included.

357 increase, with greater increases from the 2020s to the 2090s. In particular, the 99th
 358 percentile of precipitation will increase more than 50% in both dry and moderate
 359 periods in 2090s versus the 1960s. Examining inner domain grid points' annual maximum precipi-
 360 tation (Figure 11), the mean and upper tail of the annual maximum precipitation
 361 distribution both increase into the future. We expect unprecedented extreme precipita-
 362 tion (daily precipitation larger than 160 mm/day) may occur (especially in non-dry years)
 363 that will challenge the capacity of flood control equipment in NEUS.

364 **4.5 Evapotranspiration**

365 Enhanced evapotranspiration can directly reduce the net input of water from at-
 366 mosphere to land, decrease runoff and soil moisture, and increase water demands for agri-
 367 culture and ecosystems. Figure 12) shows that our future analogues exhibit greater sum-

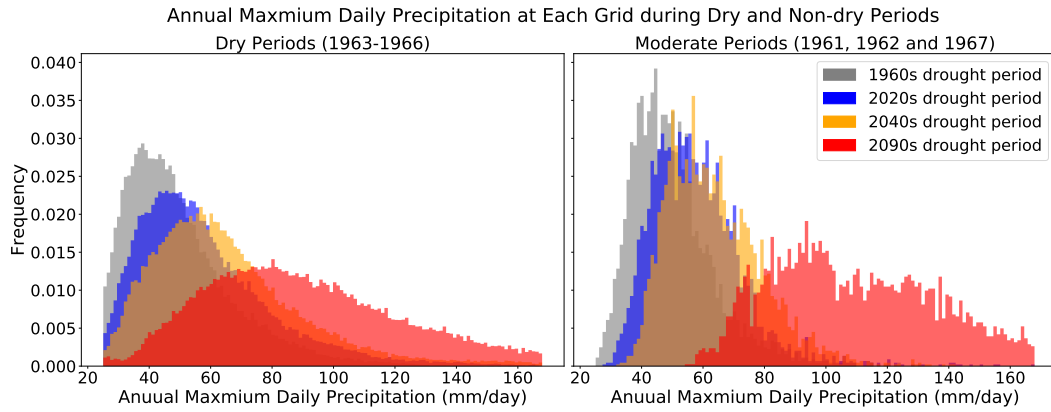


Figure 11. Annual maximum precipitation distribution of all grid points within the inner domain.

368 mertime evapotranspiration compared to winter, in accord with the spatial and tempo-
 369 ral distribution of historical precipitation (Figure 9). Of course, this is unsurprising as
 370 evapotranspiration amounts are closely related to water available. Evapotranspiration
 371 also increases more toward higher latitudes because of the warming effect, especially in
 372 wintertime. These trends hold for all dry and moderate years (Figure 9). Moderate pe-
 373 riods producing stronger evapotranspiration intensity are likely caused by more signif-
 374 icant warming and more abundant precipitation.

375 As noted earlier, precipitation increases correlate with historical precipitation. Con-
 376 sidering the strong relationship between the evapotranspiration and precipitation change,
 377 this inspires the question “how does a net precipitation (precipitation minus evapotran-
 378 spiration) change emerge?” Figure 13 shows that although evapotranspiration increases,
 379 precipitation increases more rapidly, thus producing an overall increase of net precipi-
 380 tation. Consequently, our earlier use of “wet becomes wetter” also applies to net precipi-
 381 tation, especially in winter months where correlations are more than 0.6 (and up to
 382 0.87) between historical net precipitation and its change during both dry and moderate
 383 periods. It’s further clear that the dry period summertime has much less net precipita-
 384 tion than the moderate period, suggesting that net precipitation is valid for indicating
 385 drought conditions. Note that the wet conditions of 1965 DJF was caused by a short-
 386 term abundant historical precipitation event.

387 4.6 Snowpack

388 Due to its connection to the hydrologic cycle, water supply and ecosystems in the
 389 NEUS, an understanding of future snowpack is necessary for water resource planning.
 390 Figure 14 shows a clear and rapid decrease in snowpack in this region in DJF and MAM
 391 in response to warming. Within the inner domain, seasonal regional mean snow water
 392 equivalent (SWE) was 20.56 kg/m² in 1965 DJF; however, 2095 DJF only produced 7.16
 393 kg/m² of SWE (a 61% decline). This decrease is most pronounced in the spring season
 394 (MAM); 2095 MAM exhibits a 94% drop in SWE over 1965 MAM (Figure 15). Lower
 395 latitudes are most strongly impacted as here snow is more sensitive to temperature in-
 396 creases. The result is a loss of spring snowmelt contribution to runoff (Figure 14).

397 Although there is a greater absolute SWE loss over the moderate period, the rela-
 398 tive change in the 1961 moderate year (Figure 14) is still much smaller than in the 1965
 399 dry year (Figure 14). Notably, during the 1965 dry period there is practically no histor-
 400 ical snow accumulation in spring over the northeastern states of the NEUS (Figure 14),

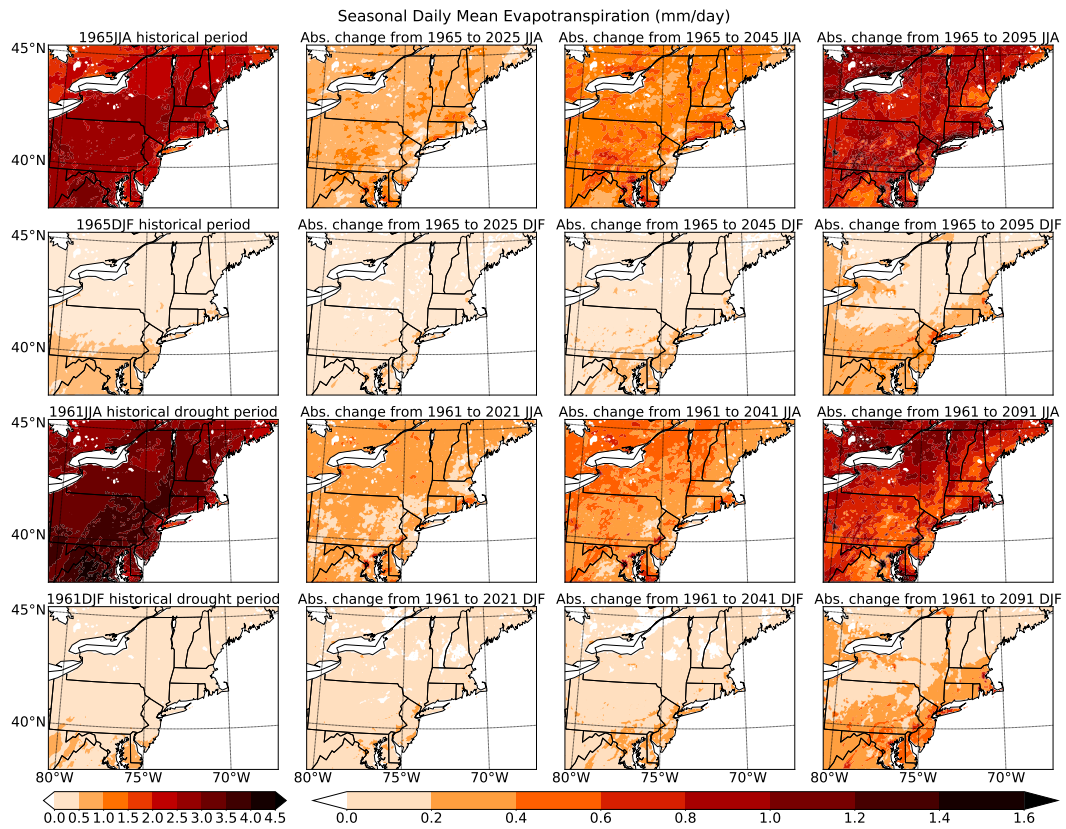


Figure 12. Seasonal mean evapotranspiration (mm/day) over the 1965 dry exemplar and 1961 moderate exemplar, and projected changes in their future analogues for the JJA and DJF seasons.

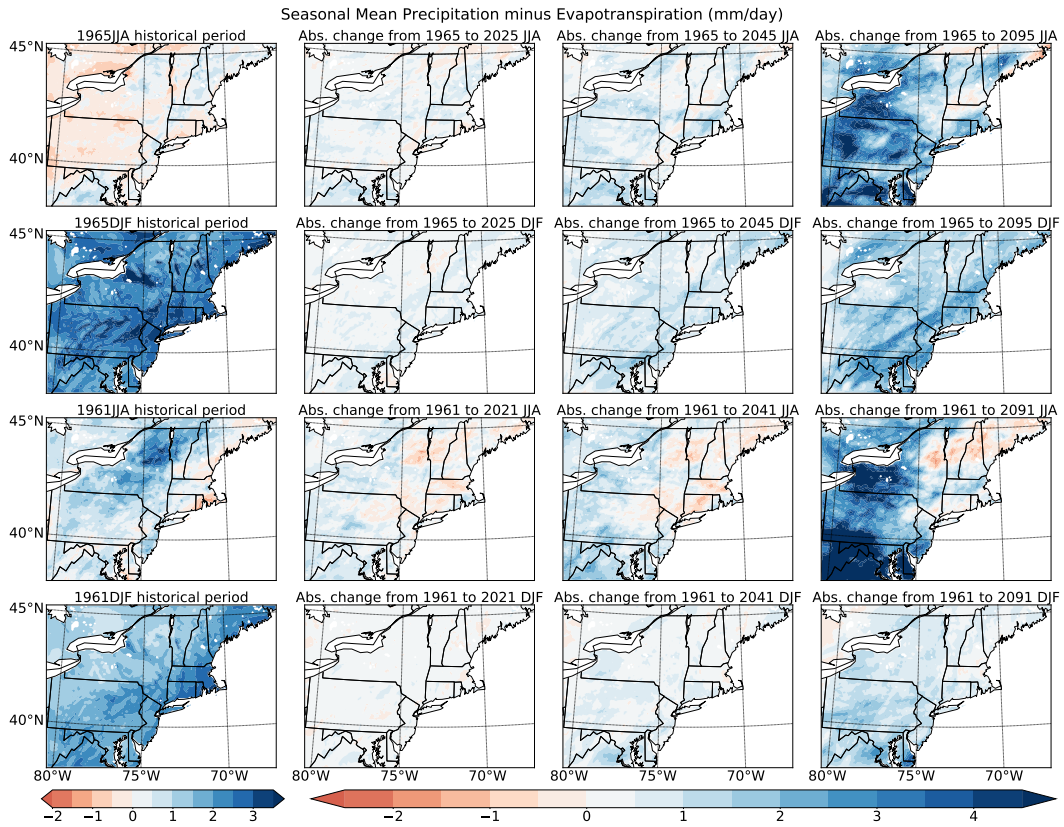


Figure 13. Seasonal mean net precipitation (mm/day) over the 1965 dry exemplar and 1961 moderate exemplar, and projected changes in their future analogues for the JJA and DJF seasons.

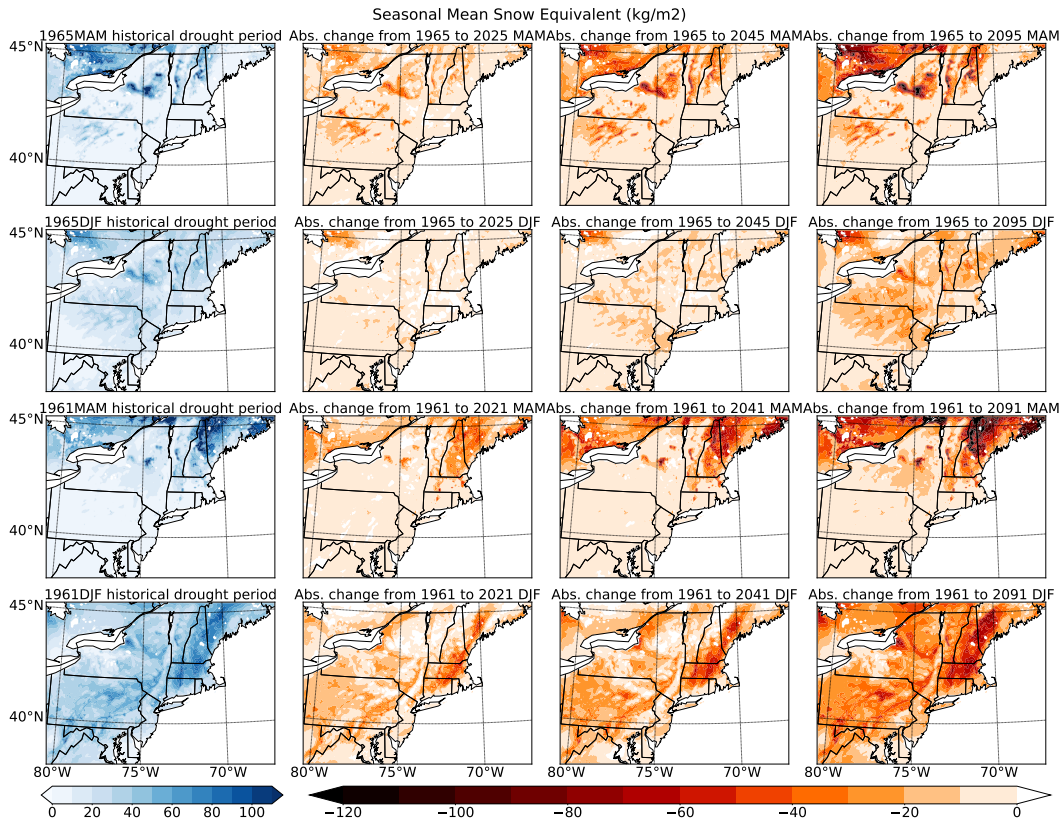


Figure 14. Seasonal mean snowpack absolute change (kg/m²) over the 1965 dry exemplar and 1961 moderate exemplar, and projected changes in their future analogues for the JJA and DJF seasons.

401 a result of low precipitation. The depleted wintertime snowpack was a major reason for
 402 the seriousness of the drought in springtime; without snowmelt the surface runoff reached
 403 record lows. Over the northeastern corner of the domain the absolute change in SWE
 404 between 1965 and its future analogue is thus fairly small, because there is essentially no
 405 snow to remove (Figure 14). On the other hand, during the moderate periods this re-
 406 gion has a healthy snowpack, which is severely depleted in the future (Figure 14).

407 4.7 Soil moisture and runoff

408 Soil moisture and runoff are two essential hydrologic variables and indicators of drought
 409 and water supply. In WRF-CLM4, soil moisture is accumulated over 10 layers; we fo-
 410 cus on the average column soil moisture, which is the average soil moisture in each layer
 411 weighted by its thickness. Seasonal mean soil moisture over the 1965 and 1961 exemplar
 412 years (and differences in their future analogues) are depicted in Figure 16. Simulated runoff
 413 is directly output by WRF and its seasonal means and future change shown in Figure
 414 17. Unsurprisingly, soil moisture trends upwards in accordance with net precipitation.
 415 Both dry and moderate periods have more soil moisture near the coast, however a sig-
 416 nificant increase can also be found during the moderate periods to the northeast. Although
 417 both net precipitation and soil moisture are generally increasing, surface runoff exhibits
 418 a decreasing trend in some regions, particularly during the dry periods, which we attribute
 419 to increasing snowmelt and frozen ground degradation and not obviously increased net
 420 precipitation (as discussed in section 4.5).

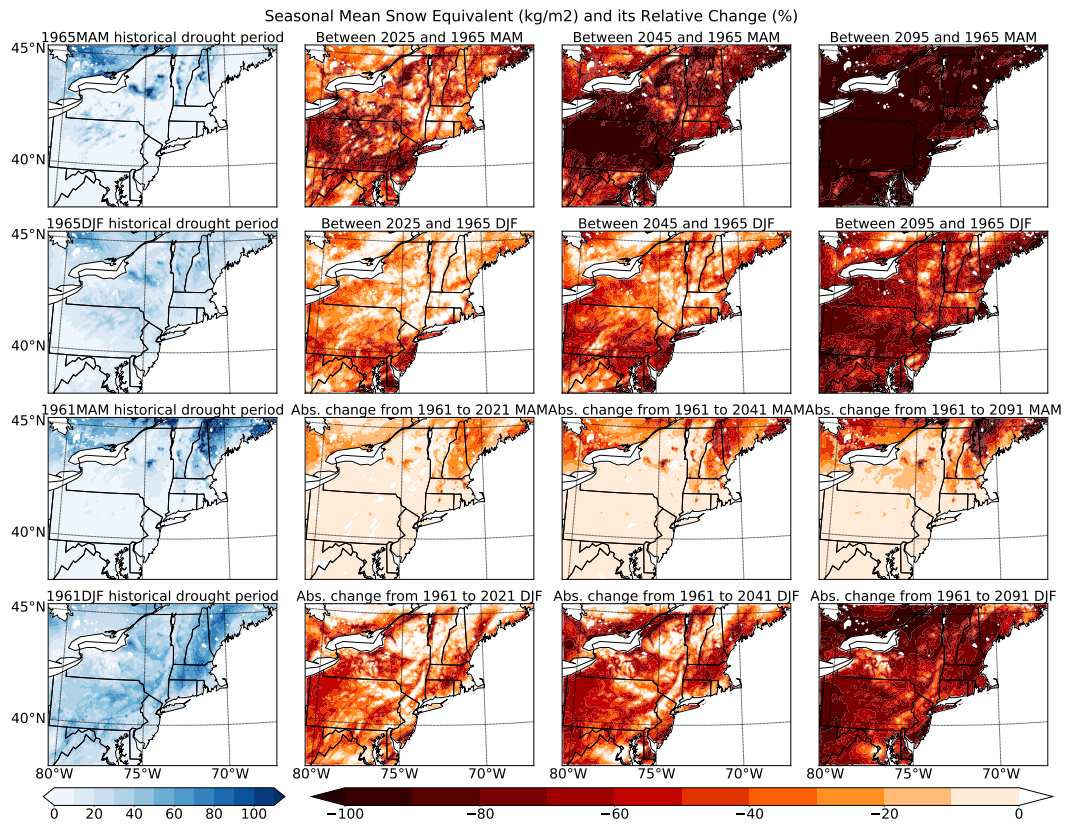


Figure 15. Seasonal mean snow water equivalent and its relative change over the 1965 dry exemplar and 1961 moderate exemplar, and projected changes in their future analogues for the JJA and DJF seasons.

421

4.7.1 Frozen ground degradation

422

423

424

425

426

427

428

429

430

431

432

Degradation of frozen ground is apparent for both the soil moisture and runoff fields regardless of time period. Frozen ground refers to permanently or seasonally frozen soil moisture, and can be assessed in terms of the number of freezing days (T. Zhang et al., 2003). Freezing of soil moisture drives up soil impermeability and reduces hydraulic conductivity, leading to a decline in soil infiltration and increase in surface runoff (more information on soil permeability in WRF-CLM4 is given in Appendix Appendix A). On the other hand, frozen ground degradation increases soil infiltration and reduces surface runoff. Frozen ground degradation is triggered by a loss of snowpack and reduction in freezing days, both of which are anticipated in a warmer climate. We argue that, particularly in DJF and MAM, frozen ground degradation is even more important for affecting soil moisture and runoff than net precipitation.

433

434

435

436

437

438

439

440

441

442

443

444

445

446

447

First, we observe that, compared with the dry years (Figures 14 and 13), moderate years experience a significant summertime net precipitation decrease and soil moisture increase simultaneously in the northeast (particularly in Canada). Certainly this would appear contradictory if net precipitation was the only driver of soil moisture change. However, the discrepancy can instead be explained by increases in snowmelt accompanied by frozen ground degradation, leading to greater infiltration to soil. Because historical snowpack was essentially zero in this region during the dry period, absolute decreases in snowpack and their recharge to soil moisture are also low in the future periods (Figure 14). But during the moderate period, abundant historical snowpack was present over the same region (Figure 14), resulting in far more snowmelt in spring and summer, and greater soil recharge and surface runoff under a warming climate. This extra recharge from snowmelt also explains why, during the moderate period, the surface runoff decrease is much smaller than during the dry period (Figure 17). It also illustrates why over the northeast, dry periods have a greater net precipitation increase but lower soil moisture increase.

448

449

450

451

452

453

454

What's more, our hypothesis that frozen ground degradation has essential impacts on moistening of the soil is evinced with the fact that there exists a pretty strong negative correlation between regional mean soil moisture change and freezing days change (-0.88) that is even larger than its correlation with regional mean net precipitation change (0.79) during the winter season of dry periods over the inner domain. And in a multivariate linear regression model, freezing degree days and net precipitation change are together strong predictors of soil moisture delta ($R^2 > 0.85$).

455

4.7.2 Shifting runoff seasonality

456

457

458

459

460

461

462

463

In general, regions whose historical temperatures are just below 0°C are the most vulnerable to frozen ground degradation, as any enhancement in temperature would prevent freezing of soil moisture. As the soils of these regions then permit greater infiltration, they are also the regions in our simulations that experience the greatest decrease in surface runoff. As a result, frozen ground degradation leaves a clear seasonal signature in the runoff field: In Figure 17 it is apparent that the regions with the most surface runoff decrease do overlap with regions of historically seasonally frozen soil, at lower latitudes in DJF and higher latitudes during MAM.

464

465

466

467

468

469

470

471

The most obvious decrease in runoff under dry conditions occurs in our New England subregion, also the most populated subregion of our domain (Figure 17), and one with significant surface water demand. Loss of snowpack and frozen ground degradation here can be implicated in producing lower runoff and more infiltration, especially in the late winter and early spring. Examination of the long term monthly mean runoff change (Figure 18) confirms our claim that the largest runoff decrease is in early spring when SWE and frost days are most reduced into the future. Over the dry period, the inner domain produces the largest historical regional monthly mean runoff in March due

472 to abundant recharge from snowmelt; however, by end-of-century, March monthly mean
 473 runoff is reduced from 0.330 to 0.155 $\mu\text{m}/\text{day}$ (more than a 50% loss). In fact, by end-
 474 of-century the surface regional runoff in the dry period peak moves from March to Au-
 475 gust in response to increasing summer precipitation. The springtime decrease in runoff
 476 is even more obvious within the New England subregion (Figure S7), where reductions
 477 in frozen days and snow water equivalent are more pronounced (Figure 15). Shifting of
 478 surface runoff away from spring has important consequences for agriculture – as discussed
 479 in section 2, the water shortage from the 1960s drought was at its most severe in the early
 480 spring due to agricultural demands.

481 4.8 Drought indices

482 From our earlier analysis, a generally warming climate with greater precipitation,
 483 evaporation and snowmelt are likely for a future analogue to the 1960s drought. How-
 484 ever, overall wetter mean conditions doesn't necessarily imply that such a drought comes
 485 with fewer challenges. After all, the impacts of drought are complex and the product of
 486 multiple variables. Given wetter conditions are accompanied by increased temperatures
 487 and evapotranspiration, which in turn magnify the need for water, it's important to con-
 488 sider compound indices of drought as applied to historical and future conditions.

489 Standardized Precipitation Index (SPI) is a widely used family of drought indica-
 490 tors designed to capture the intensity of meteorological drought conditions (Hayes et al.,
 491 2002; Svoboda & Fuchs, 2016). Specifically, the metrics SPI_n quantify the accumulated
 492 departure from the mean of n consecutive months' accumulated precipitation. Smaller
 493 values of n are relevant for short-term droughts and larger values for long-term droughts.
 494 However, a key limitation of the basic SPI metric is that it cannot account for evapo-
 495 transpiration, preventing it from capturing moisture demand, and making it unsuitable
 496 for detecting flash droughts. Therefore, here we examine a modified version of SPI which
 497 instead uses net precipitation in place of actual precipitation (hereafter referred to as stan-
 498 dardized net precipitation index, SNPI). We choose not to employ Standardized Precip-
 499 itation Evapotranspiration Index (SPEI) (Vicente-Serrano et al., 2010) since WRF-CLM4
 500 provides an accurate and internally-consistent version of evapotranspiration directly (Lawrence
 501 et al., 2011; Xu et al., 2020), whereas SPEI would require an empirical calculation of po-
 502 tential evapotranspiration (ET₀). Past work has also illustrated that over sufficiently wet
 503 regions SNPI and SPEI are largely indistinguishable (Beguería et al., 2014; Joetzjer et
 504 al., 2012). Details on the calculation of SNPI are provided in Appendix ???. Our inter-
 505 pretation of SNPI values is analogous to the interpretation of SPI given in Table 2 (Guttman,
 506 1999).

507 To begin, trends of long-term drought conditions are examined using SNPI₂₄. The
 508 1960s drought is clearly visible in Figure 19 (top), and appears as the driest period in
 509 the past 100 years. The year 1965 exhibits the lowest annual mean SNPI₂₄ value, in ac-
 510 cord with the claim that 1965 was the driest of the past century. These results validate
 511 the use of SNPI and its effectiveness for identifying drought conditions. Looking to the
 512 future, although both precipitation and evapotranspiration increase substantially, an-
 513 nual mean regional SNPI₂₄ at 2025 is only about -1, barely classifying as a drought. Un-
 514 der further warming, 2045 actually becomes anomalously wet – with SNPI₂₄ in 2041 ac-
 515 tually surpassing any historical value of SNPI₂₄. At the end of this century (2090s), SNPI₂₄
 516 in every year is larger than 2, indicative that even under the same dynamical conditions
 517 of the 1960s, the climate will be unprecedented compared to historical. These results gen-
 518 erally suggest that the threat from long-term meteorological drought over the next cen-
 519 tury will be greatly diminished.

520 Although the climatological shift towards wetter conditions will mitigate long-term
 521 drought, we can still ask if extreme drought conditions are similarly mitigated on shorter
 522 time scales? In fact, our simulations suggest the answer is “probably not.” Specifically,

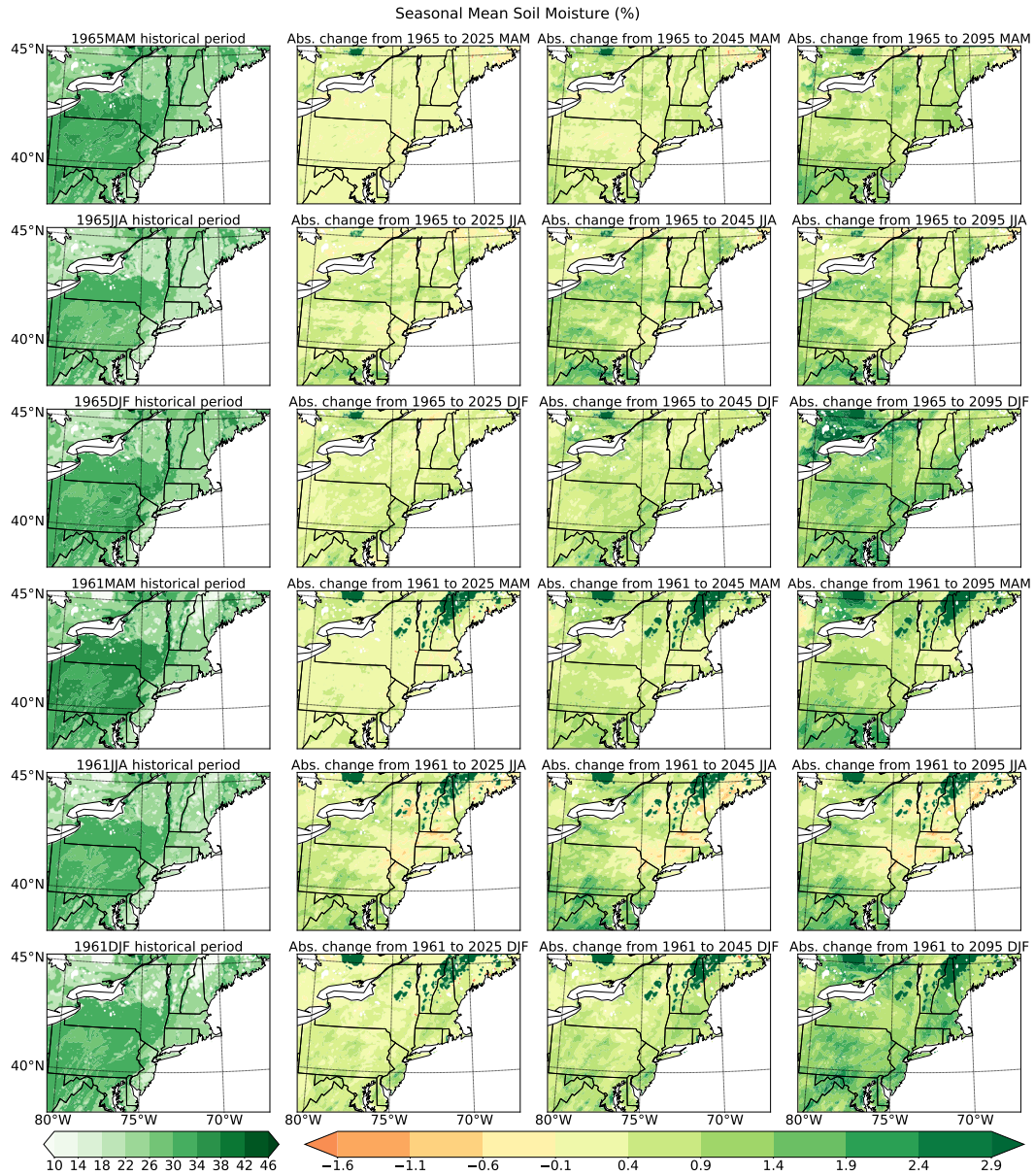


Figure 16. Seasonal mean soil moisture change (%) over the 1965 dry exemplar and 1961 moderate exemplar, and projected changes in their future analogues for the MAM, JJA, and DJF seasons.

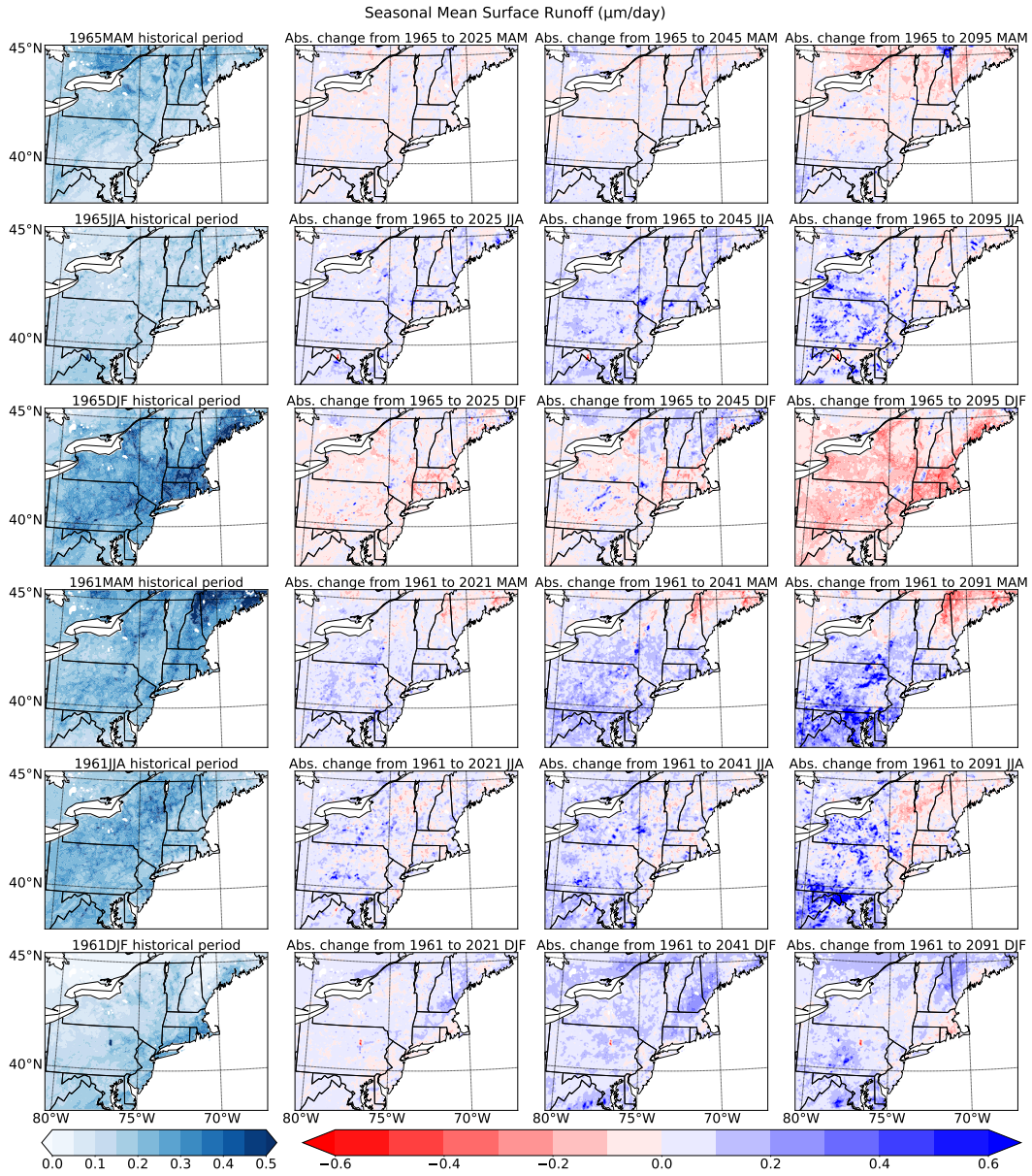


Figure 17. Seasonal mean runoff change (mm/day) over the 1965 dry year and 1961 moderate year, and projected changes in their future analogues for the MAM, JJA, and DJF seasons.

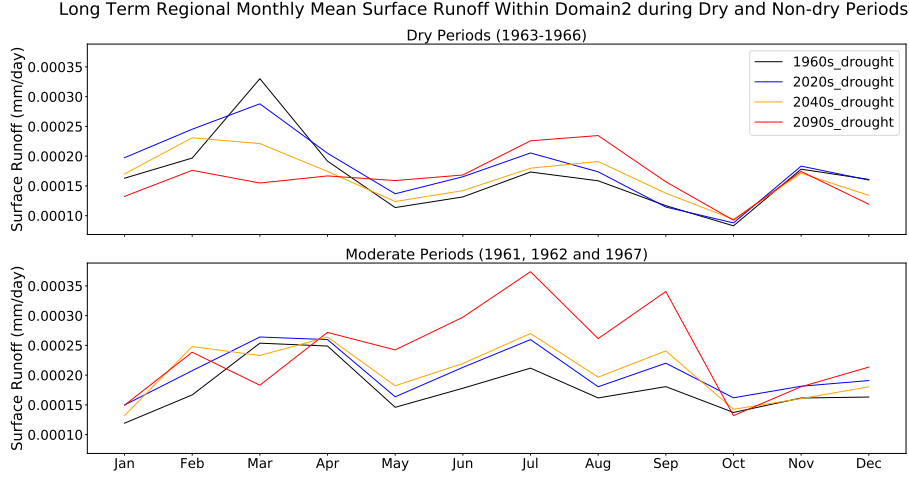


Figure 18. Regional long-term monthly mean runoff within the inner domain during dry years and moderate years.

Table 2. SNPI Classification following (Guttman, 1999).

SNPI Value	Conditions
$SNPI \geq 2$	Extremely Wet
$2 > SNPI \geq 1.5$	Very Wet
$1.5 > SNPI \geq 1$	Moderately Wet
$1 > SNPI > -1$	Nearly Normal
$-1.5 < SNPI \leq -1$	Moderately Dry
$-2 < SNPI \leq -1.5$	Very Dry
$SNPI \leq -2$	Extremely Dry

we calculate the SNPI1 of 1960s historical drought period (1963-1966) with that of the three future drought scenarios. Figure 19 (bottom) clearly shows that even as wetter months experience enhanced net precipitation, short-term extreme drought conditions persist. In fact, in the most extremely dry months (e.g. May 1964 and 1965), dryness is largely unchanged. Although the mean of SNPI1 during this period rises from -0.33 to 0.61, in accord with the general wetting trend, the standard deviation of SNPI1 also soars from 0.95 to 1.31, indicative of enhanced drought variability. This reflects enhanced climatological differences between dry and wet periods. More importantly, drought tends to happen more quickly – that is, a likely increase in the frequency *flash drought* (Christian et al., 2019). For example, April 2094 has a SNPI1 larger than 2 followed by a sudden drop to less than -3 in May; extremely dry conditions develop from extremely wet conditions in only one month! Suddenly adapting to dry conditions in such a short time would be an immense challenge for the region’s water managers and stakeholders.

5 Conclusions

In this paper, the unprecedented 1960s NEUS drought is simulated as it occurred historically and subject to anticipated climate change from the early (2020-2027), middle (2040-2047) and late (2090-2097) 21st century. To do so, the pseudo-global warming methodology is employed in WRF-CLM4: dynamical boundary conditions are iden-

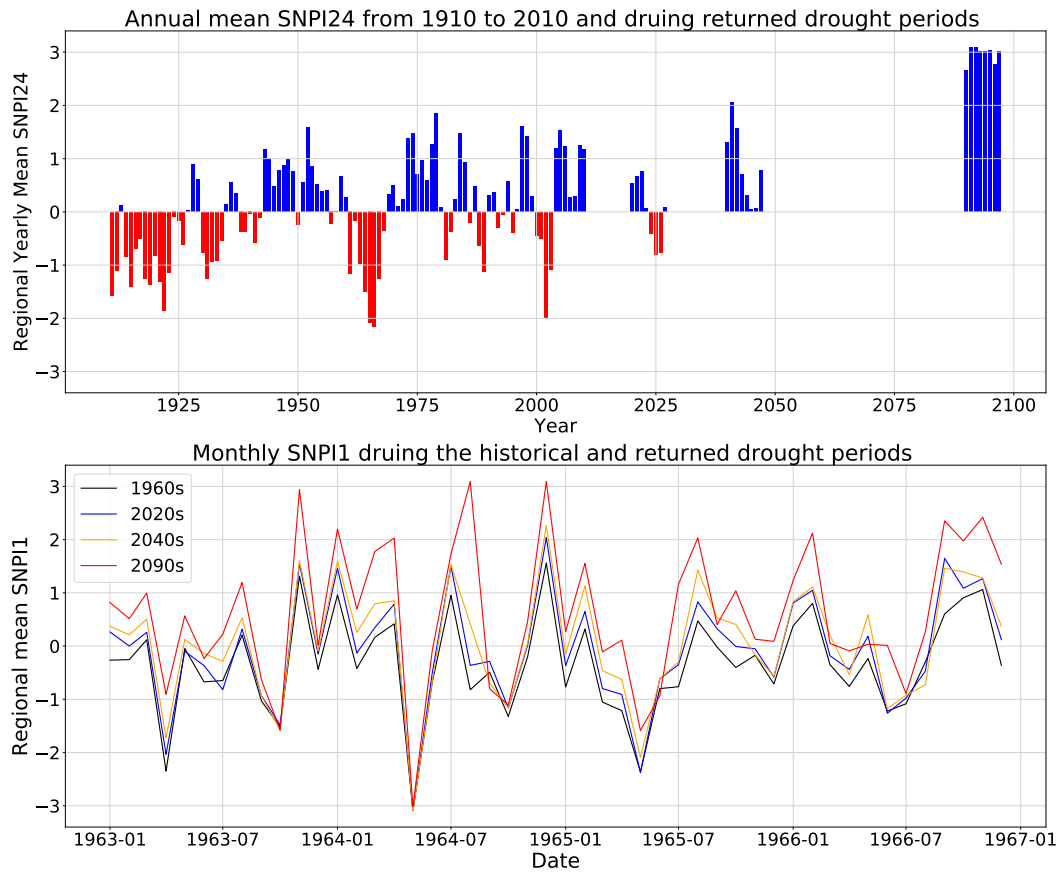


Figure 19. Regional annual mean SNPI24 and monthly mean SNPI1 within the New England subregion over historical and future periods.

541 tical to the historical period, while thermodynamics (atmospheric temperature, sea sur-
542 face temperature and greenhouse gas concentration) are modified using the mean of four
543 highly performant CMIP6 models under RCP8.5. Overall, our simulations reveal that
544 although there is a significant wetting trend due to the overall increase in net precipi-
545 tation (precipitation minus evapotranspiration) and moistening of the soil, this wetting
546 is only apparent during non-dry months, while dry months with negative net precipita-
547 tion are generally unchanged. This enhanced hydrologic variability has the potential to
548 accelerate the development of drought, and make it possible for an extreme flash drought
549 to rapidly emerge from wet conditions. Further, additional socioeconomic challenges will
550 arise because of the surges in extreme hot days, unprecedented extreme heavy precip-
551 itation events, obvious shifts of climate patterns, and far less runoff in early spring as
552 a result of frozen ground degradation and loss of snowpack. Our main findings are as fol-
553 lows:

554 First, as the prescribed lateral boundary conditions constrain temperatures, sim-
555 ulated years within each period have nearly the same regional mean warming. Compared
556 with the 1960s period, the annual regional warming overland is 1.92-2.01°C in the 2020s,
557 3.16-3.27°C in the 2040s, and 6.74-6.87°C in the 2090s. However, significant spatial and
558 temporal differences in warming emerge. For instance, cold regions warm faster than warm
559 regions – a result that is more obvious at winter. Surging extreme heat days also make
560 heat waves a potential problem over the NEUS in the future. Compared with more mod-
561 erate periods, dry periods will experience a greater increase in both mean and extreme
562 values of annual maximum daily temperature. Whereas each year of the historical pe-
563 riod had less than 10 extreme heat days, the 2020s period had 7 - 30 extreme heat days,
564 the 2040s had 14 - 40 days, and the 2090s had 52 - 79 days. Potential risks related to
565 extreme hot weather include heatstroke and death.

566 Second, a clear annual mean precipitation increase emerges over the NEUS into the
567 future (Figure 3). Regional annual mean precipitation increases by approximately 15%,
568 27% and 70% at the beginning, middle and end of the 21st century. Precipitation increases
569 more in regions with higher historical mean precipitation, especially in the winter in both
570 dry and non-dry periods (with spatial correlation around 0.6). After accounting for in-
571 creased evapotranspiration, most regions maintain a positive net precipitation change.
572 A standardized drought index (SNPI24) is employed to show the gradual transforma-
573 tion from extremely dry to extremely wet conditions: Qualitatively, annual mean con-
574 ditions in the 2020s are moderately dry, nearly neutral in the 2040s, and extremely wet
575 in the 2090s. However, this does not imply extremely dry conditions at the monthly scale
576 will vanish in the future: Because precipitation increase is only apparent in wet months,
577 months with negative net precipitation are largely unchanged from historical. Consequently,
578 our simulations suggest “wet months get wetter but dry months get drier (or are unchanged).”
579 Consequently, net precipitation variability increases in a warming climate. Higher tem-
580 peratures and enhanced evapotranspiration may produce flashier flash droughts and re-
581 quire longer lead times on water planning. Our simulations produce instances of extremely
582 dry months ($\text{SNPI1} \leq -2$) that immediately follow extremely wet conditions ($\text{SNPI1} \geq$
583 2) in the 2090s. Such sudden drying could be devastating to agriculture, especially dur-
584 ing the growing season. Drought monitoring systems working on shorter timescales that
585 further incorporate short-term forecasting would be desirable in this case, though lim-
586 itations on predictability could limit their value.

587 Third, increased precipitation amount and variability will drive more frequent and
588 intense extreme storm events. Averaged over the simulation region, the probability of
589 annual maximum precipitation exceeding 100 mm/day increases from 7.16% in the 1960s
590 to 25.19% in the 2090s during dry periods, and from 6.28% at 1960s to 36.45% in the
591 2090s during moderate periods. The most extreme (99th percentile) regional mean pre-
592 cipitation intensifies by more than 58% and 51% by the end of this century during mod-
593 erate and dry periods, respectively. Extreme precipitation brings with it a high risk of

594 flooding needed investments in protective infrastructure. Extreme precipitation from trop-
 595 ical cyclones wasn't touched on in this paper, although Hurricane Donna was captured
 596 in our simulation period; as in (Reed et al., 2020), we anticipate that climate change will
 597 increase precipitation, intensity, and size of these storms.

598 Fourth, significant warming in colder regions of the domain induces a substantial
 599 decrease in the number of regional mean freezing days and snowpack totals. We see a
 600 60% decrease in the mean number of days with minimum daily temperature below 0°C,
 601 and a greater than 75% loss of snow water equivalent in the 2090s winter period versus
 602 historical. Consequently, we anticipate substantial degradation of frozen ground, which
 603 will increase soil infiltration and result in more water recharging to soil instead of sur-
 604 face runoff. More precipitation will occur as rainfall instead of snow, and snowmelt will
 605 happen earlier, essentially eliminating spring snowpack. Consequently surface runoff will
 606 decrease in spring due to lack of recharge from snowmelt.

607 Fifth, although it's intuitive that increases in net precipitation would produce more
 608 soil moisture and surface runoff, we argue that frozen ground degradation plays a larger
 609 role here. In support of this claim, summers of the moderate period feature a northeast-
 610 ern region with obviously reduced net precipitation, but the most significant increase in
 611 soil moisture. This directly opposes expectations if only net precipitation were implicated
 612 in moister soil. However, we find that reduced snowpack and freezing days permits greater
 613 infiltration from snow melting – in fact, during the winter season of dry periods, a strong
 614 negative correlation (-0.88) emerges between the change in the regional mean number
 615 of freezing days and soil moisture. This correlation is even larger than the positive cor-
 616 relation between the regional net precipitation change and soil moisture change.

617 Finally, we project a decrease in surface runoff during the winter and spring be-
 618 cause of less snowmelt, along with increased infiltration to the soil due to the frozen ground
 619 degradation. Our simulations suggest March surface runoff decreases more than 50% in
 620 the 2090s dry periods compared with the 1960s drought period. This raises the specter
 621 of water shortages resulting from insufficient early spring runoff. From our simulations,
 622 we project the growing season to be the most vulnerable to anticipated future changes.
 623 In conjunction with increased water demand from higher temperatures, a reduction in
 624 available water poses great socioeconomic challenges.

625 This study primarily focuses on seasonal and regional scale changes, but ignores
 626 the consequences of particular weather events that occur on finer temporal and spatial
 627 scales. Given that the finest spatial and temporal resolution of our simulation is 9 km
 628 and 6 hours, our dataset could enable deeper exploration into specific events, along with
 629 their underlying process drivers. For example, this data could enable a better understand-
 630 ing of the strongest hurricane during 1960s period – Hurricane Donna – and its mani-
 631 festation in the future in this region. Questions also remain about the potential for flash
 632 drought in this region under more general dynamical conditions, and how the 1960s drought
 633 compares to potentially more extreme droughts of the future for this region. Finally, given
 634 the simplifications made in CLM, there are substantial uncertainties in historical and
 635 projected surface and groundwater hydrology in these simulations; consequently it would
 636 be insightful to examine the response of a process-based hydrologic model to forcing data
 637 from these simulations.

638 **Appendix A Soil degradation in WRF-CLM4**

639 In the land model we used (WRF-CLM4), the soil infiltration factor is defined by
 640 equation A1. We can see that, when there is less freezing days, for each soil layer i , the
 641 ice contents ($w_{ice,i}$) will decrease and the liquid water contents ($w_{liq,i}$) will increase so
 642 that the impermeable fraction $f_{frz,i}$ will consequently decrease too which indicates that

643 the soil layers are less impermeable and there will be more infiltration to recharge the
 644 soil moisture (Oleson et al., 2010) .

$$f_{frz,i} = \frac{\exp[-\alpha(1 - \frac{w_{ice,i}}{w_{ice,i} + w_{liq,i}})] - \exp(-\alpha)}{1 - \exp(-\alpha)} \quad (A1)$$

645 where $f_{frz,i}$ is the impermeable fraction which impacts the infiltration capacity, $w_{ice,i}$
 646 and $w_{liq,i}$ ($kg \times m^{-2}$) are the ice and liquid water contents of soil layer i . $\alpha = 3$ is an ad-
 647 justable scale-dependent parameter.

648 Appendix B Calculation of standardized net precipitation index (SNPI)

In this study SNPI is calculated analogous to SPI (Hayes et al., 2002; Svoboda & Fuchs, 2016), with a small modification for robustness. Generally, SPI is calculated by fitting the raw data to a gamma distribution, and then transforming it to be normally distributed. But under extremely dry conditions, evapotranspiration may exceed the precipitation giving a negative net precipitation, and so violate the requirements of the Gamma distribution. Thus we follow (Adams, 2017) and adjust the net precipitation data to make sure all data is non-negative prior to the fit:

$$\text{Net Precipitation}_{n,i} = \text{Net Precipitation}_{n,i} - \min(\text{Net Precipitation}) \quad (B1)$$

649 The calibration of SPI is sensitive to the quantity of data employed (following (Guttman,
 650 1999) more than 50 years data is recommended). Since our WRF-CLM4 simulations are
 651 each only 8 years long, we instead combine the historical precipitation and evapotran-
 652 spiration data from CERA20C R7 from 1910 to 2010 with our 1960s historical simula-
 653 tion to build a 101 years historical net precipitation time series data as the calibration
 654 period of SNPI for 3 future simulations (2020s, 2040s and 2090s). Namely, with the as-
 655 sumption that net precipitation nearly following the gamma distribution, all our data
 656 will be transformed to a normal distribution from a gamma distribution with the param-
 657 eters calculated based on the historical data from 1910 to 2010. Our rationale for only
 658 using the historical period to calibrate the SNPI is to prevent our future drought pro-
 659 jections from impacting the SNPI of the historical drought. To ensure our simulation data
 660 are consistent with CERA20C R7, WRF-CLM4 simulations are corrected by adding the
 661 regional mean differences between CERA20C R7 and WRF over the historical period
 662 (1961-1967).

663 Acknowledgments

664 We would like to thank Melissa Bukovsky, Rachel McCrary, and Zexuan Xu for their
 665 insights into proper execution of these regional simulations. We would also like to thank
 666 Shu-Hua Chen for granting us computer time to perform some of these simulations. This
 667 research was supported by the RGMA program area(s) in the U.S. Department of En-
 668 ergy's Office of Biological and Environmental Research as part of the multi-program, col-
 669 laborative Integrated Coastal Modeling (ICoM) project. PAU was supported by Depart-
 670 ment of Energy Office of Science award number DE-SC0016605, "A Framework for Im-
 671 proving Analysis and Modeling of Earth System and Intersectoral Dynamics at Regional
 672 Scales (HyperFACETS)." This project is also supported by the National Institute of Food
 673 and Agriculture, U.S. Department of Agriculture, hatch project under California Agri-
 674 cultural Experiment Station project accession no. 1016611. We acknowledge the World
 675 Climate Research Programme, which, through its Working Group on Coupled Modelling,
 676 coordinated and promoted CMIP6. We thank the climate modeling groups for produc-
 677 ing and making available their model output, the Earth System Grid Federation (ESGF)
 678 for archiving the data and providing access, and the multiple funding agencies who sup-

port CMIP6 and ESGF. The WRF model simulation data mentioned in this paper is available from ZENODO at <https://doi.org/10.5281/zenodo.4310852>.

References

- Adams, J. (2017). *climate-indices, an open source python library providing reference implementations of commonly used climate indices*. https://github.com/monocongo/climate_indices.
- Andreadis, K. M., & Lettenmaier, D. P. (2006). Trends in 20th century drought over the continental United States. *Geophysical Research Letters*, *33*(10).
- Barksdale, H. C. (1968). *The northeast water supply crisis of the 1960's* (Tech. Rep.). Reston, VA: US Government Printing Office.
- Barksdale, H. C., O'Bryan, D., & Schneider, W. J. (1966). *Effect of drought on water resources in the Northeast* (Tech. Rep.). Reston, VA: US Government Printing Office.
- Beguéría, S., Vicente-Serrano, S. M., Reig, F., & Latorre, B. (2014). Standardized precipitation evapotranspiration index (SPEI) revisited: parameter fitting, evapotranspiration models, tools, datasets and drought monitoring. *International Journal of Climatology*, *34*(10), 3001–3023.
- Bretherton, C. S., & Park, S. (2009). A new moist turbulence parameterization in the Community Atmosphere Model. *Journal of Climate*, *22*(12), 3422–3448.
- Burns, D. A., Klaus, J., & McHale, M. R. (2007). Recent climate trends and implications for water resources in the Catskill Mountain region, New York, USA. *Journal of Hydrology*, *336*(1-2), 155–170.
- Byrne, M. P., & O’Gorman, P. A. (2015). The response of precipitation minus evapotranspiration to climate warming: Why the “wet-get-wetter, dry-get-drier” scaling does not hold over land. *Journal of Climate*, *28*(20), 8078–8092.
- Case, J. L., Crosson, W. L., Kumar, S. V., Lapenta, W. M., & Peters-Lidard, C. D. (2008). Impacts of high-resolution land surface initialization on regional sensible weather forecasts from the WRF model. *Journal of Hydrometeorology*, *9*(6), 1249–1266.
- Chou, C., & Neelin, J. D. (2004). Mechanisms of global warming impacts on regional tropical precipitation. *Journal of Climate*, *17*(13), 2688–2701.
- Christian, J. I., Basara, J. B., Otkin, J. A., Hunt, E. D., Wakefield, R. A., Flanagan, P. X., & Xiao, X. (2019). A methodology for flash drought identification: Application of flash drought frequency across the United States. *Journal of Hydrometeorology*, *20*(5), 833–846.
- Cook, E. R., & Jacoby, G. C. (1977). Tree-ring-drought relationships in the Hudson Valley, New York. *Science*, *198*(4315), 399–401.
- Dai, A., Trenberth, K. E., & Qian, T. (2004). A global dataset of Palmer Drought Severity Index for 1870–2002: Relationship with soil moisture and effects of surface warming. *Journal of Hydrometeorology*, *5*(6), 1117–1130.
- DeGaetano, A. T. (1999). A temporal comparison of drought impacts and responses in the New York city metropolitan area. *Climatic Change*, *42*(3), 539–560.
- Demaria, E. M., Palmer, R. N., & Roundy, J. K. (2016). Regional climate change projections of streamflow characteristics in the Northeast and Midwest US. *Journal of Hydrology: Regional Studies*, *5*, 309–323.
- Donat, M. G., Lowry, A. L., Alexander, L. V., O’Gorman, P. A., & Maher, N. (2016). More extreme precipitation in the world’s dry and wet regions. *Nature Climate Change*, *6*(5), 508–513.
- European Centre for Medium-Range Weather Forecasts. (2016). *Coupled ECMWF Re-Analysis system of the 20th-century*. <https://www.ecmwf.int/en/forecasts/datasets/reanalysis-datasets/cera-20c>.
- Frumhoff, P. C., McCarthy, J. J., Melillo, J. M., Moser, S. C., & Wuebbles, D. J. e. a. (2007). Confronting climate change in the US Northeast: Sci-

- ence, impacts, and solutions. *Confronting climate change in the US Northeast: science, impacts, and solutions.*
- Ganetis, S. A., & Colle, B. A. (2015). The thermodynamic and microphysical evolution of an intense snowband during the northeast US blizzard of 8–9 February 2013. *Monthly Weather Review*, *143*(10), 4104–4125.
- Guttman, N. B. (1999). Accepting the standardized precipitation index: a calculation algorithm 1. *JAWRA Journal of the American Water Resources Association*, *35*(2), 311–322.
- Hayes, M. J., Alvord, C., & Lowrey, J. (2002). *Drought indices*. National Drought Mitigation Center, University of Nebraska.
- Hayhoe, K., Wake, C., Anderson, B., Liang, X.-Z., Maurer, E., Zhu, J., ... Wuebbles, D. (2008). Regional climate change projections for the Northeast USA. *Mitigation and Adaptation Strategies for Global Change*, *13*(5-6), 425–436.
- Hayhoe, K., Wake, C. P., Huntington, T. G., Luo, L., Schwartz, M. D., Sheffield, J., ... DeGaetano, A. e. a. (2007). Past and future changes in climate and hydrological indicators in the US Northeast. *Climate Dynamics*, *28*(4), 381–407.
- Hobbs, J. J. (2008). *World regional geography*. Nelson Education.
- Hoegh-Guldberg, O., Jacob, D., Bindi, M., Brown, S., Camilloni, I., Diedhiou, A., ... Guiot, J. e. a. (2018). Impacts of 1.5 °C global warming on natural and human systems. *Global warming of 1.5° C. An IPCC Special Report*.
- Huntington, T. G., Hodgkins, G. A., Keim, B. D., & Dudley, R. W. (2004). Changes in the proportion of precipitation occurring as snow in New England (1949–2000). *Journal of Climate*, *17*(13), 2626–2636.
- Iacono, M. J., Delamere, J. S., Mlawer, E. J., Shephard, M. W., Clough, S. A., & Collins, W. D. (2008). Radiative forcing by long-lived greenhouse gases: Calculations with the AER radiative transfer models. *Journal of Geophysical Research: Atmospheres*, *113*(D13).
- Janes, B. E., & Brumbach, J. J. (1965). The 1964 Agriculture Drought in Connecticut. *University of Connecticut*.
- Jiménez, P. A., Dudhia, J., González-Rouco, J. F., Navarro, J., Montávez, J. P., & García-Bustamante, E. (2012). A revised scheme for the WRF surface layer formulation. *Monthly Weather Review*, *140*(3), 898–918.
- Jin, J., Miller, N. L., & Schlegel, N. (2010). Sensitivity study of four land surface schemes in the WRF model. *Advances in Meteorology*, *2010*.
- Joetzjer, E., Douville, H., Delire, C., Ciais, P., Decharme, B., & Tyteca, S. (2012). Evaluation of drought indices at interannual to climate change timescales: a case study over the Amazon and Mississippi river basins. *Hydrology & Earth System Sciences Discussions*, *9*(11).
- Kharin, V. V., Zwiers, F. W., Zhang, X., & Hegerl, G. C. (2007). Changes in temperature and precipitation extremes in the IPCC ensemble of global coupled model simulations. *Journal of Climate*, *20*(8), 1419–1444.
- Kimura, F., Kitoh, A., Sumi, A., Asanuma, J., & Yatagai, A. (2007). Downscaling of the global warming projections to Turkey. *The Final Report of ICCAP*, *10*.
- Krakauer, N. Y., Lakhankar, T., & Hudson, D. (2019). Trends in Drought over the Northeast United States. *Water*, *11*(9), 1834.
- Lawrence, D. M., Oleson, K. W., Flanner, M. G., Thornton, P. E., Swenson, S. C., Lawrence, P. J., ... others (2011). Parameterization improvements and functional and structural advances in version 4 of the Community Land Model. *Journal of Advances in Modeling Earth Systems*, *3*(1).
- Lindsey, R., & Dahlman, L. (2020). *Climate Change: Global Temperature*. National Oceanic and Atmospheric Administration.
- Lyon, B., Christie-Blick, N., & Gluzberg, Y. (2005). Water Shortages, Development, and Drought in Rockland County, New York. *JAWRA Journal of the American Water Resources Association*, *41*(6), 1457–1469.

- 786 Melillo, J. M., Richmond, T., & Yohe, G. e. a. (2014). Climate change impacts in
787 the United States. *Third National Climate Assessment*, 52.
- 788 Moser, S. C., Kasperson, R. E., Yohe, G., & Agyeman, J. (2008). Adaptation to
789 climate change in the Northeast United States: opportunities, processes, con-
790 straints. *Mitigation and Adaptation Strategies for Global Change*, 13(5-6),
791 643–659.
- 792 Namias, J. (1966). Nature and possible causes of the northeastern United States
793 drought during 1962–65. *Mon. Wea. Rev.*, 94(9), 543–554.
- 794 Neale, R. B., Chen, C.-C., Gettelman, A., Lauritzen, P. H., Park, S., Williamson,
795 D. L., ... Lamarque, J.-F. e. a. (2010). Description of the NCAR community
796 atmosphere model (CAM 5.0). *NCAR Tech. Note*, 1(1), 1–12.
- 797 NOAA. (2020). *Heat Index definition by NOAA*. [https://www.weather.gov/
798 safety/heat-index](https://www.weather.gov/safety/heat-index).
- 799 of Economic Analysis, U. B. (2016). Gross domestic product (GDP) by state (mil-
800 lions of current dollars). *US Bureau of Economic Analysis*.
- 801 Oleson, K. W., Lawrence, D. M., Gordon, B., Flanner, M. G., Kluzek, E., Peter, J.,
802 ... others (2010). *Technical description of version 4.0 of the Community Land
803 Model (CLM)*. Citeseer.
- 804 Pfahl, S., O’Gorman, P. A., & Fischer, E. M. (2017). Understanding the regional
805 pattern of projected future changes in extreme precipitation. *Nature Climate
806 Change*, 7(6), 423–427.
- 807 Powers, J. G., Klemp, J. B., Skamarock, W. C., Davis, C. A., Dudhia, J., Gill,
808 D. O., ... Peckham, S. E. e. a. (2017). The weather research and forecast-
809 ing model: Overview, system efforts, and future directions. *Bulletin of the
810 American Meteorological Society*, 98(8), 1717–1737.
- 811 Reed, K. A., Stansfield, A., Wehner, M., & Zarzycki, C. (2020). Forecasted attri-
812 bution of the human influence on hurricane florence. *Science Advances*, 6(1),
813 eaaw9253.
- 814 Rothfus, L. P., & Headquarters, N. S. R. (1990). The heat index equation (or, more
815 than you ever wanted to know about heat index). *Fort Worth, Texas: National
816 Oceanic and Atmospheric Administration, National Weather Service, Office of
817 Meteorology*, 9023.
- 818 Seager, R., Naik, N., & Vecchi, G. A. (2010). Thermodynamic and dynamic mech-
819 anisms for large-scale changes in the hydrological cycle in response to global
820 warming. *Journal of Climate*, 23(17), 4651–4668.
- 821 Seager, R., Pederson, N., Kushnir, Y., Nakamura, J., & Jurburg, S. (2012). The
822 1960s drought and the subsequent shift to a wetter climate in the Catskill
823 Mountains region of the New York City watershed. *Journal of Climate*,
824 25(19), 6721–6742.
- 825 Skamarock, W. C., Klemp, J. B., Dudhia, J., Gill, D. O., Barker, D. M., Wang, W.,
826 & Powers, J. G. (2008). 2005: A description of the advanced research WRF
827 version 2. In *NCAR Tech. Note*.
- 828 Srivastava, A., Grotjahn, R., & Ullrich, P. (2020). Evaluation of historical CMIP6
829 model simulations of extreme precipitation over contiguous US regions.
830 *Weather and Climate Extremes*, 100268.
- 831 Strzepek, K., Yohe, G., Neumann, J., & Boehlert, B. (2010). Characterizing changes
832 in drought risk for the United States from climate change. *Environmental Re-
833 search Letters*, 5(4), 044012.
- 834 Svoboda, M., & Fuchs, B. (2016). Handbook of drought indicators and indices.
835 Integrated drought management programme (IDMP), integrated drought man-
836 agement tools and guidelines series 2. *World Meteorological Organization and
837 Global Water Partnership, Geneva, Switzerland*, 52.
- 838 Ullrich, P., Xu, Z., Rhoades, A., Dettinger, M., Mount, J., Jones, A., & Vahmani,
839 P. (2018). California’s drought of the future: A midcentury recreation of the
840 exceptional conditions of 2012–2017. *Earth’s Future*, 6(11), 1568–1587.

- 841 Van den Dool, H., Huang, J., & Fan, Y. (2003). Performance and analysis of the
842 constructed analogue method applied to US soil moisture over 1981–2001.
843 *Journal of Geophysical Research: Atmospheres*, *108*(D16).
- 844 Vicente-Serrano, S. M., Beguería, S., & López-Moreno, J. I. (2010). A multiscalar
845 drought index sensitive to global warming: the standardized precipitation
846 evapotranspiration index. *Journal of Climate*, *23*(7), 1696–1718.
- 847 Xu, X., Li, X., Wang, X., He, C., Tian, W., Tian, J., & Yang, L. (2020). Estimat-
848 ing daily evapotranspiration in the agricultural-pastoral ecotone in Northwest
849 China: A comparative analysis of the Complementary Relationship, WRF-
850 CLM4. 0, and WRF-Noah methods. *Science of The Total Environment*,
851 138635.
- 852 Zhang, G. J., & McFarlane, N. A. (1995). Role of convective scale momentum trans-
853 port in climate simulation. *Journal of Geophysical Research: Atmospheres*,
854 *100*(D1), 1417–1426.
- 855 Zhang, T., Barry, R., Knowles, K., Ling, F., & Armstrong, R. (2003). Distribution
856 of seasonally and perennially frozen ground in the Northern Hemisphere. In
857 *Proceedings of the 8th International Conference on Permafrost* (Vol. 2, pp.
858 1289–1294).